Experimental and theoretical study of novel aminobenzamide–aminonaphthalimide fluorescent dyads with a FRET mechanism

Ángel L. García,[1] Adrián Ochoa-Terán,[1]* Antonio Tirado-Guízar,[1] Jesús Jara-Cortés,[2]* Georgina Pina-Luis,[1] Hisila Santacruz Ortega,[3] Victoria Labastida-Galván,[4] Mario Ordoñez,[4] Jorge Peón[5]

[1] Centro de Graduados e Investigación en Química, Tecnológico Nacional de México/IT de Tijuana. Tijuana, Baja California, México.

[2] Unidad Académica de Ciencias Básicas e Ingenierías, Universidad Autónoma de Nayarit. Tepic, Nayarit, México.

[3] Departamento de Investigación en Polímeros y Materiales, Universidad de Sonora. Hermosillo, Sonora, México.

[4] Centro de Investigaciones Químicas-(IICBA), Universidad Autónoma del Estado de Morelos. Cuernava, Morelos, México.

[5] Instituto de Química, Universidad Nacional Autónoma de México. Ciudad de México, México

*Correspondence e-mail: adrian.ochoa@tectijuana.edu.mx, josejc@uan.edu.mx

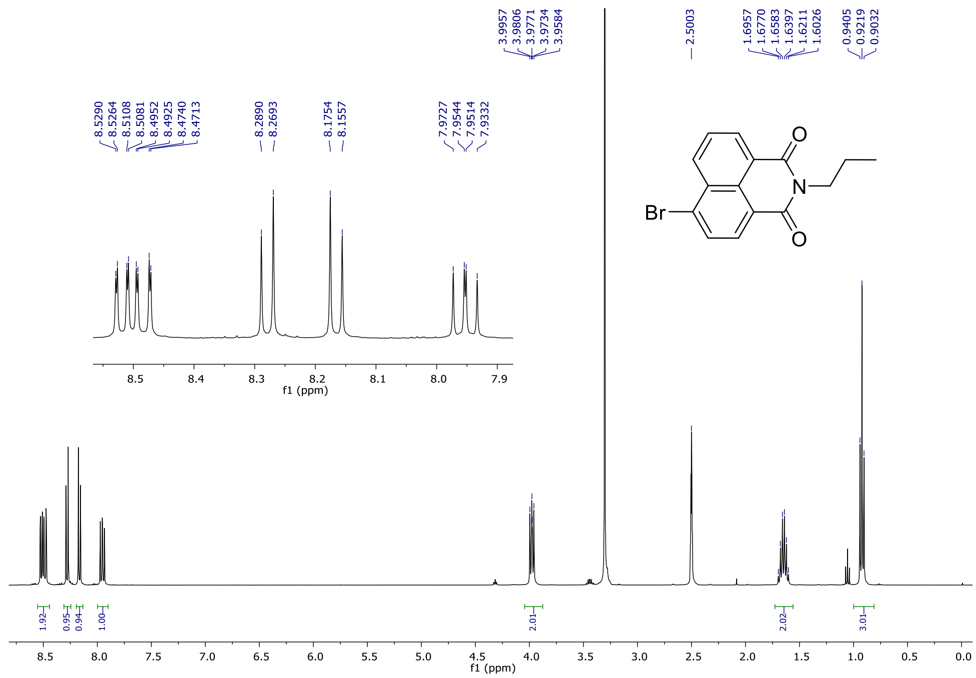

Figure S1. ^{1}H NMR spectrum of 6-bromo-2-propyl-1H-benzo[de]isoquinoline-1,3(2H)-dione **1** obtained in DMSO-d_6.

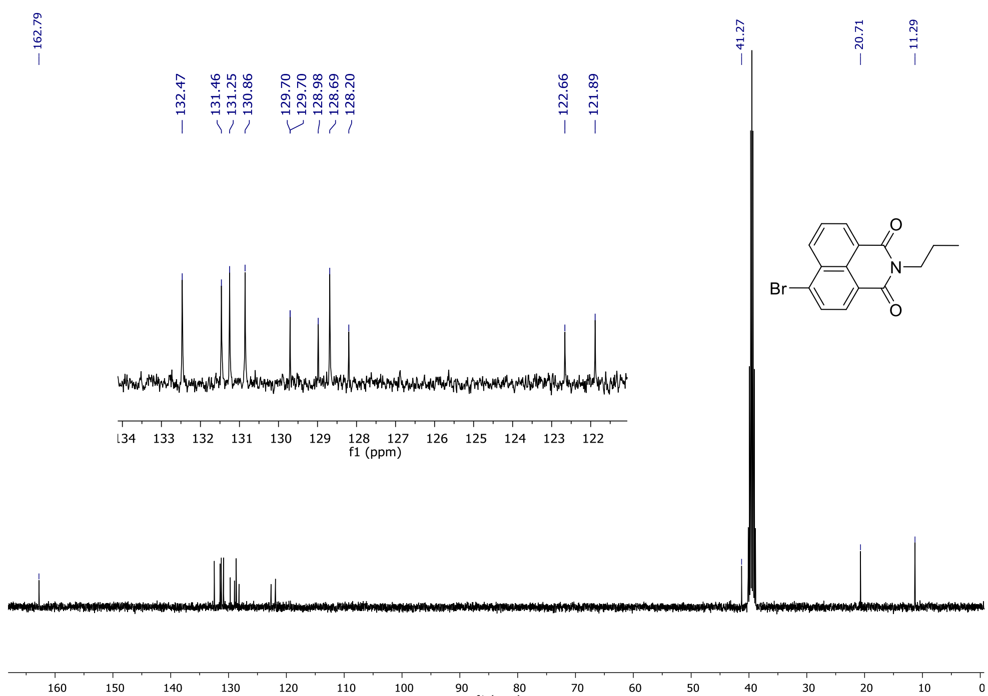

Figure S2. ^{13}C NMR spectrum of 6-bromo-2-propyl-1H-benzo[de]isoquinoline-1,3(2H)-dione **1** obtained in DMSO-*d6*.

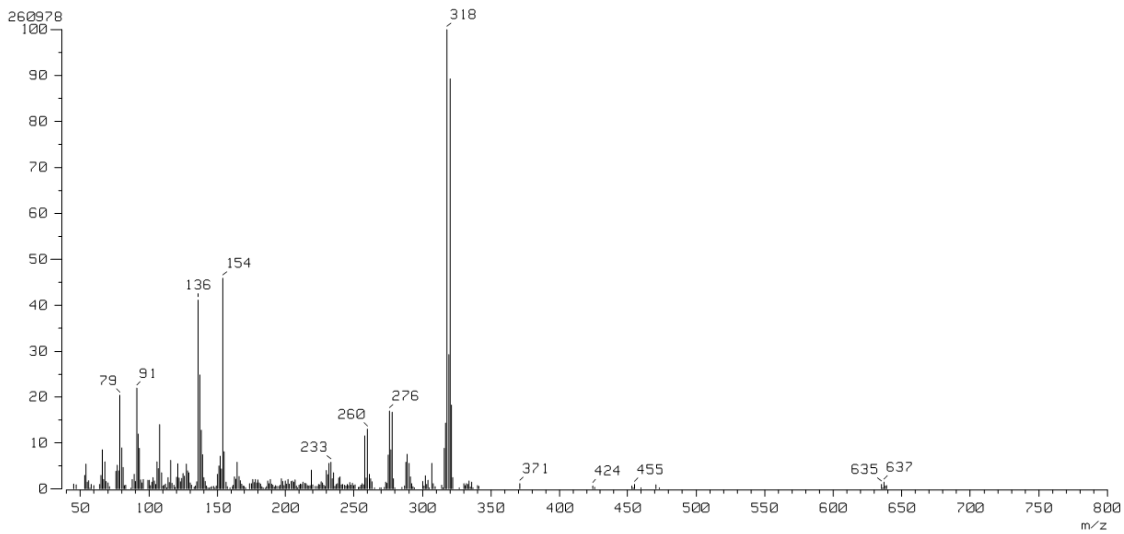

Figure S3. MS(FAB+) for **1**.

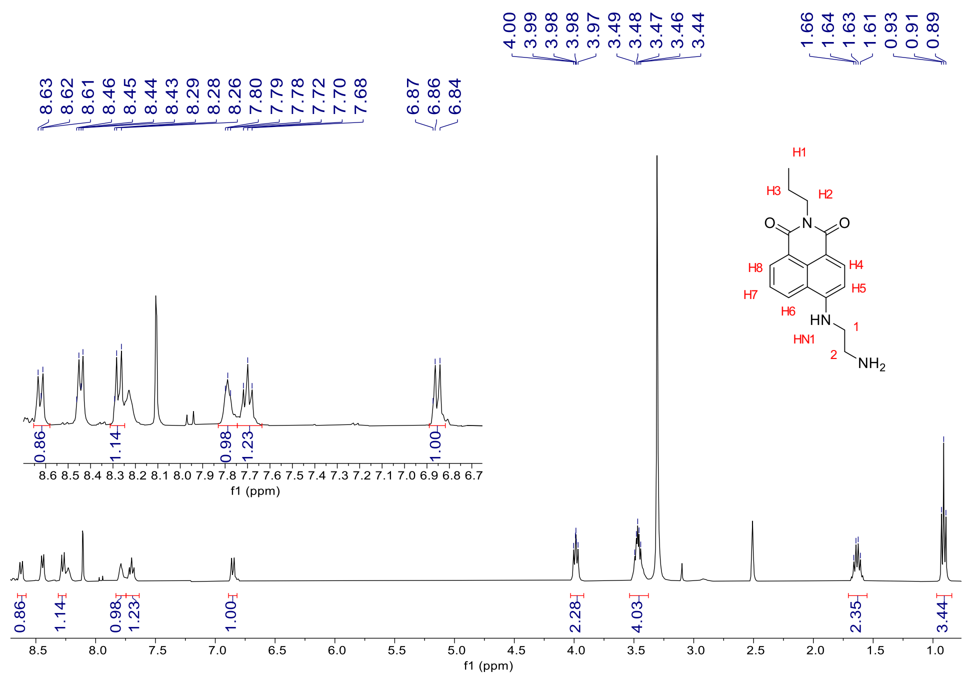

Figure S4. ^{1}H NMR spectrum of **2a** obtained in DMSO-d_6.

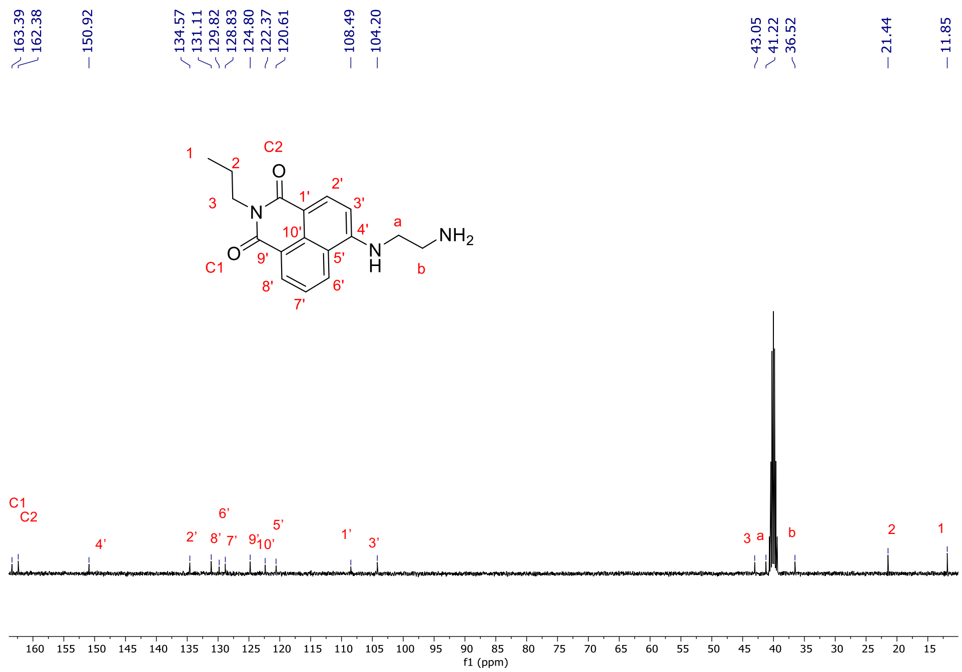

Figure S5. ^{13}C NMR spectrum of **2a** obtained in DMSO-d_6.

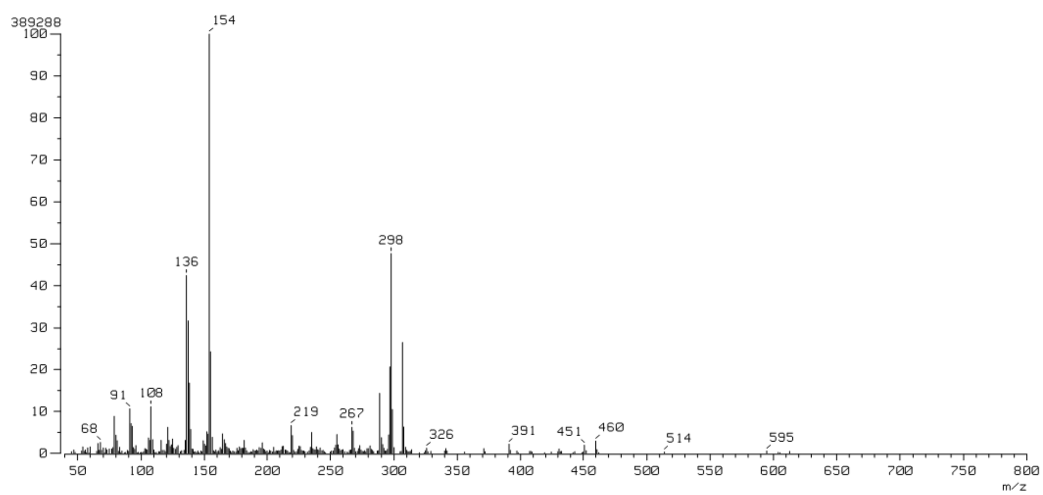

Figure S6. MS(FAB+) for **2a**.

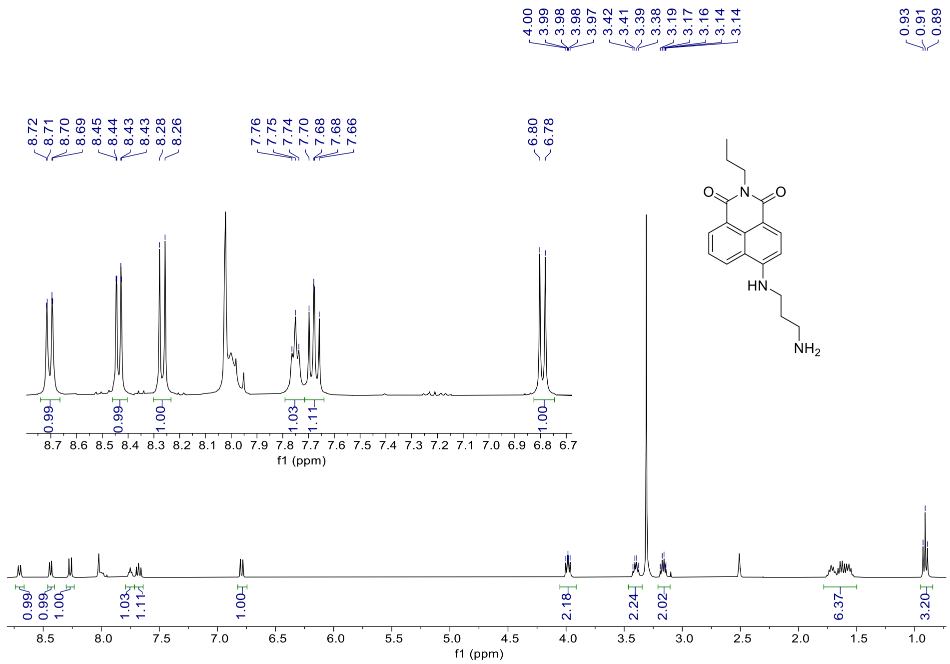

Figure S7. ^{1}H NMR spectrum of **2b** obtained in DMSO-d_6.

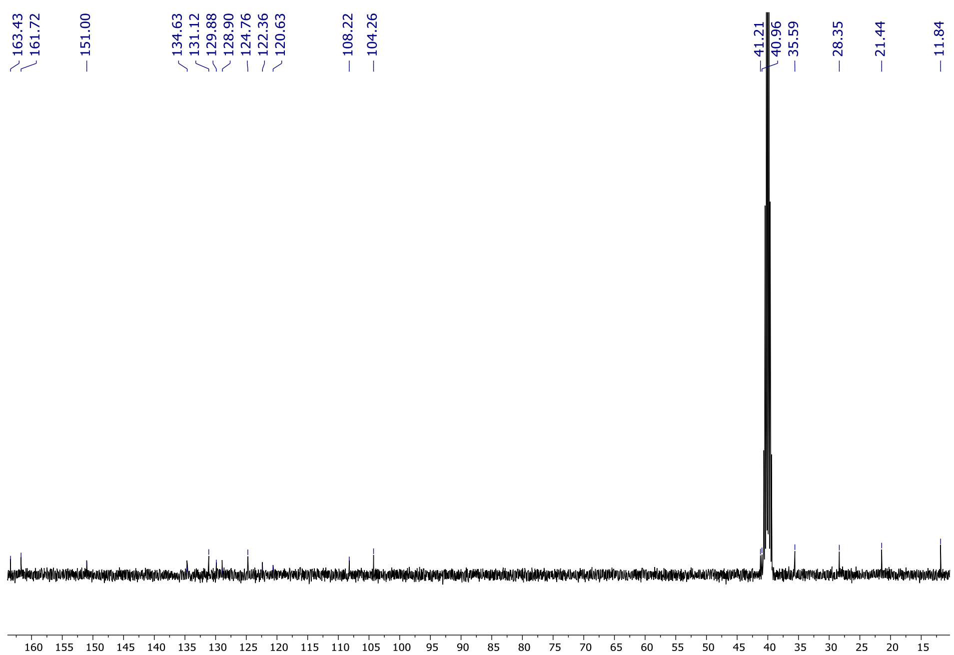

Figure S8. ^{1}H NMR spectrum of **2b** obtained in DMSO-d_6.

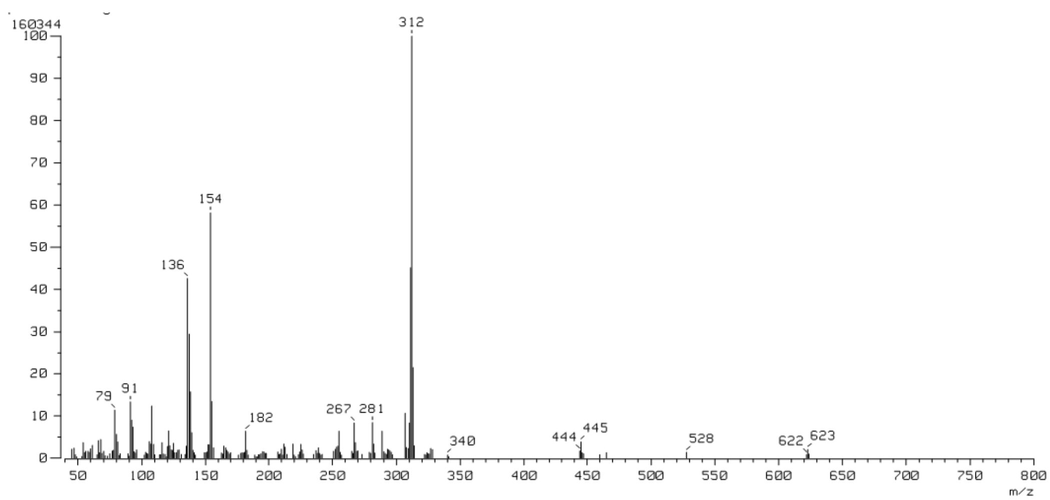

Figure S9. MS(FAB+) for **2b**.

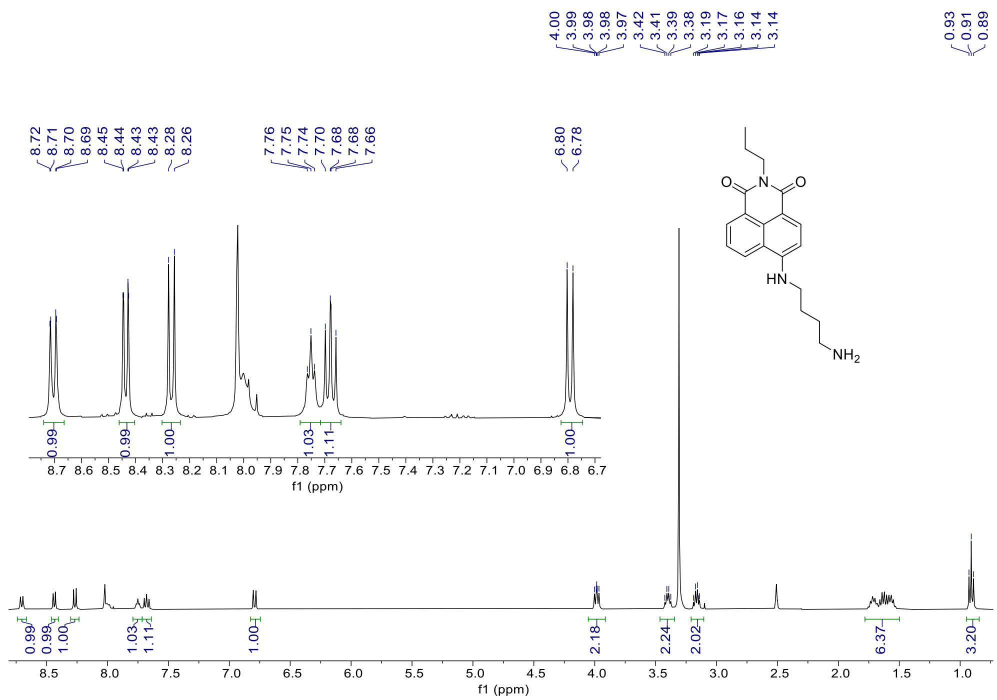

Figure S10. [1]H NMR spectrum of **2c** obtained in DMSO-d_6.

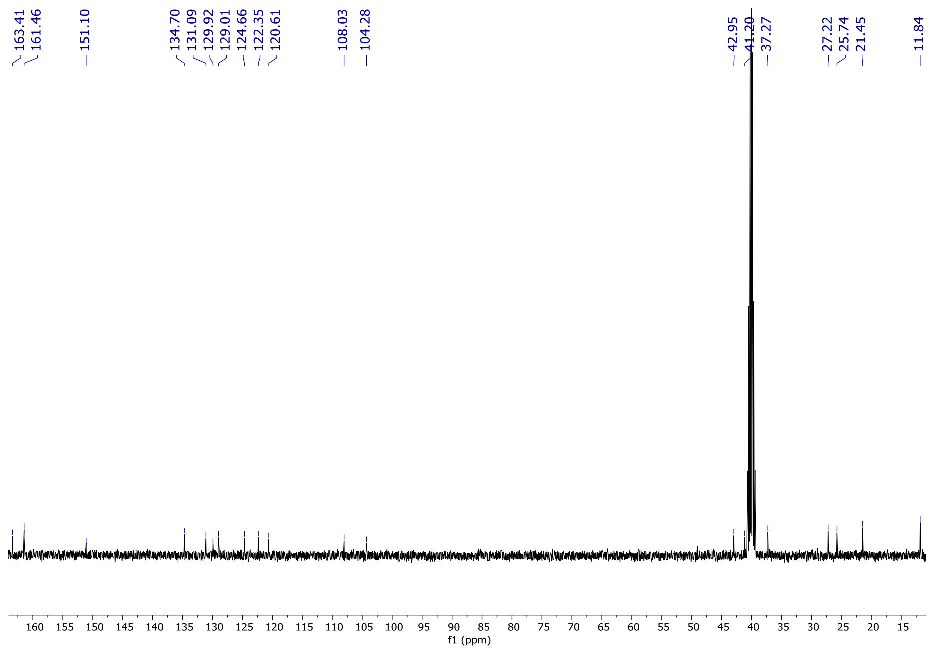

Figure S11. ^{13}C NMR spectrum of **2c** obtained in DMSO-d_6.

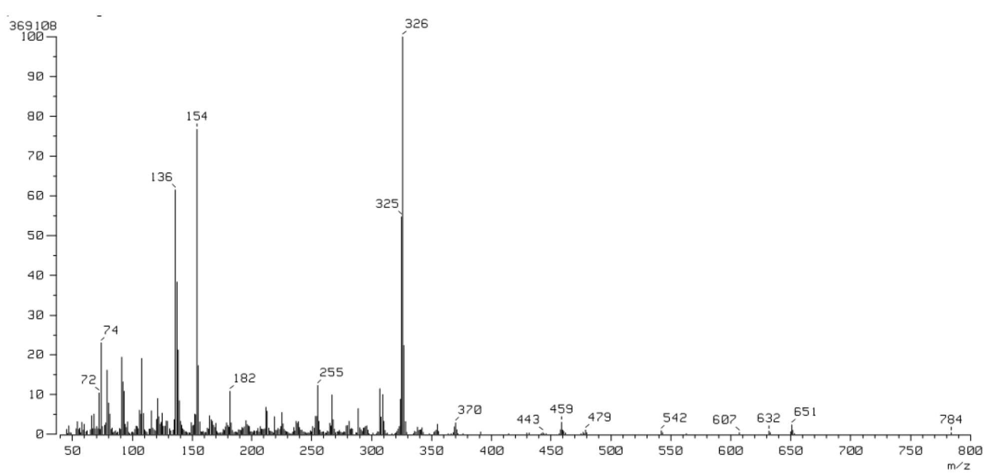

Figure S12. MS(FAB+) for **2c**.

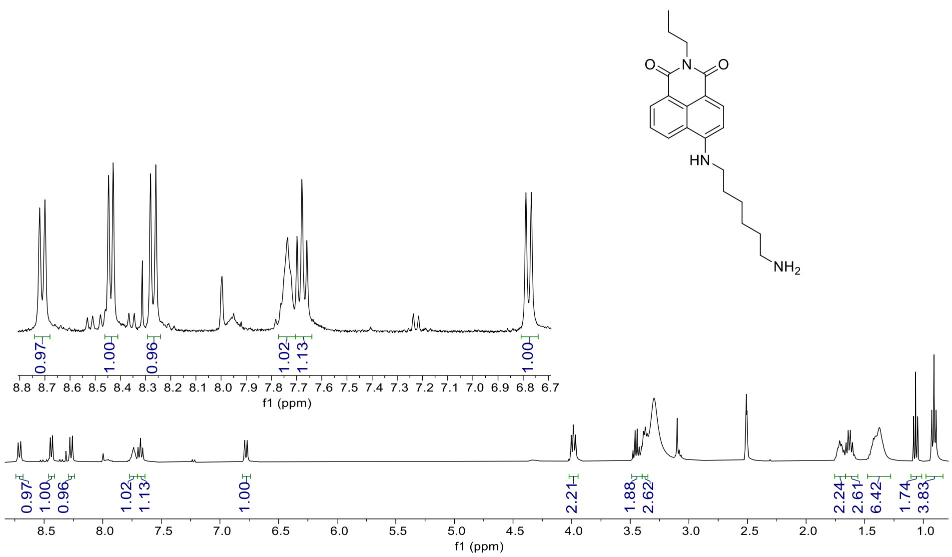

Figure S13. ^{1}H NMR spectrum of **2d** obtained in DMSO-d_6.

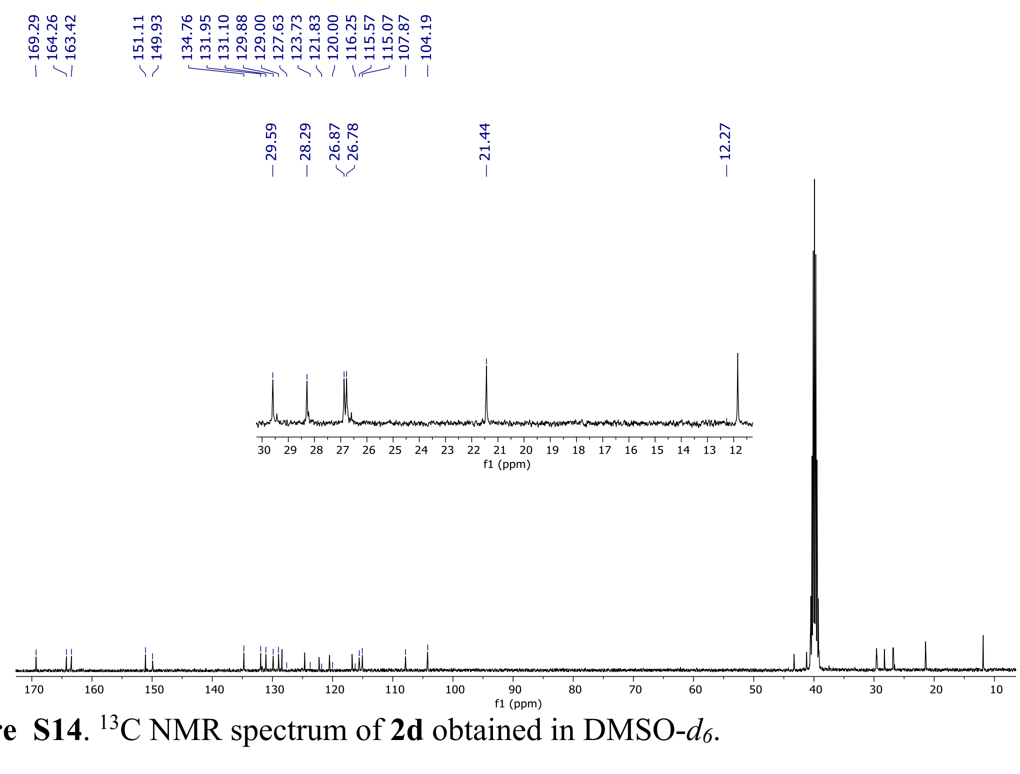

Figure S14. ^{13}C NMR spectrum of **2d** obtained in DMSO-d_6.

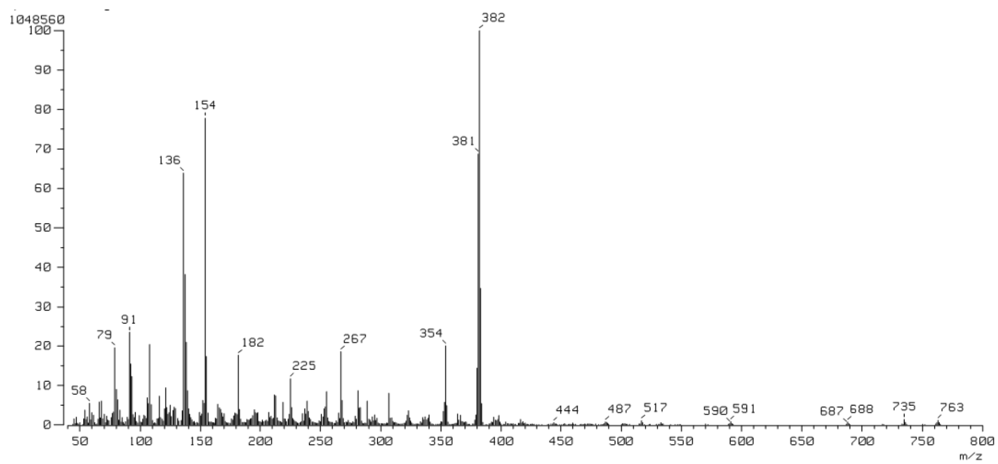

Figure S15. MS(FAB+) for **2d**.

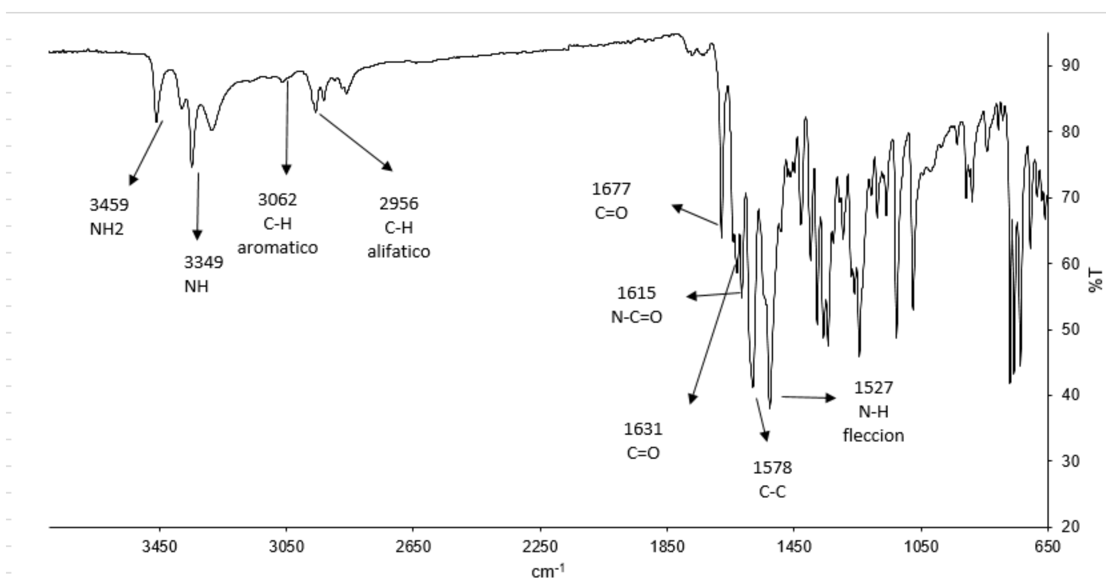

Figure S16. FTIR spectrum of **3a**.

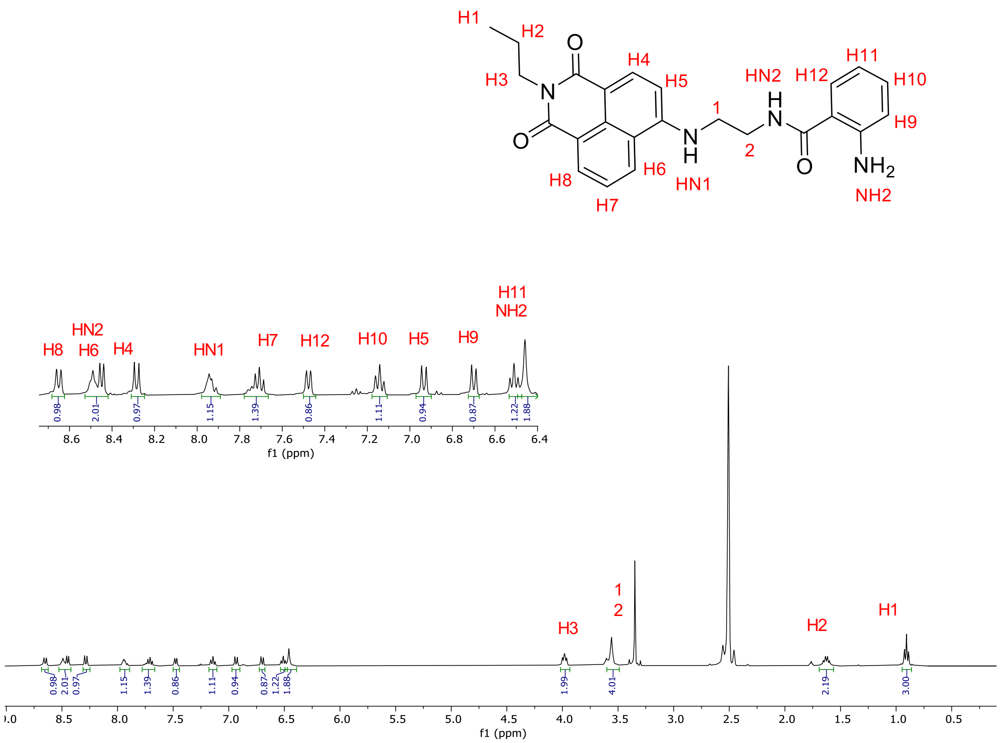

Figure S17. ^{1}H NMR spectrum of **3a** obtained in DMSO-d_6.

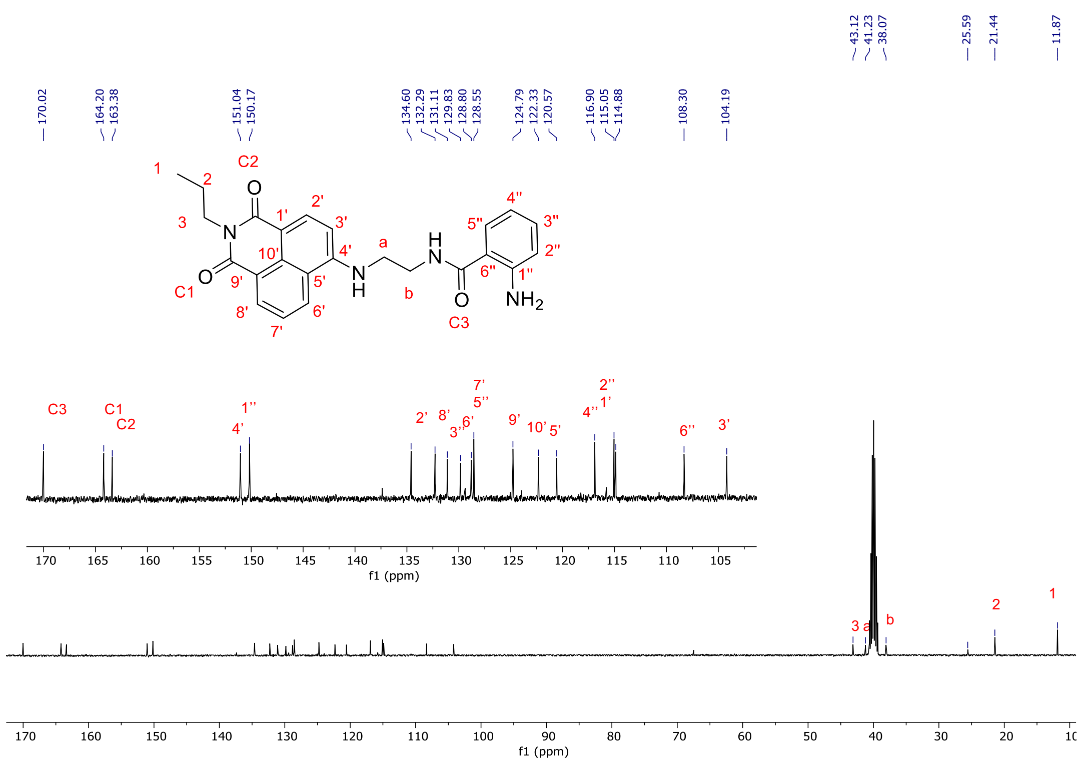

Figure S18. ^{13}C NMR spectrum of **3a** obtained in DMSO-d_6.

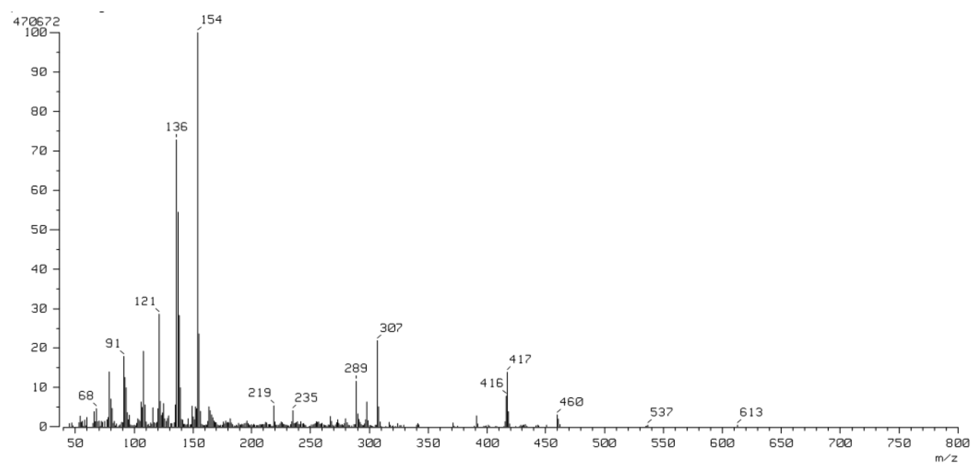

Figure S19. MS(FAB+) for **3a**.

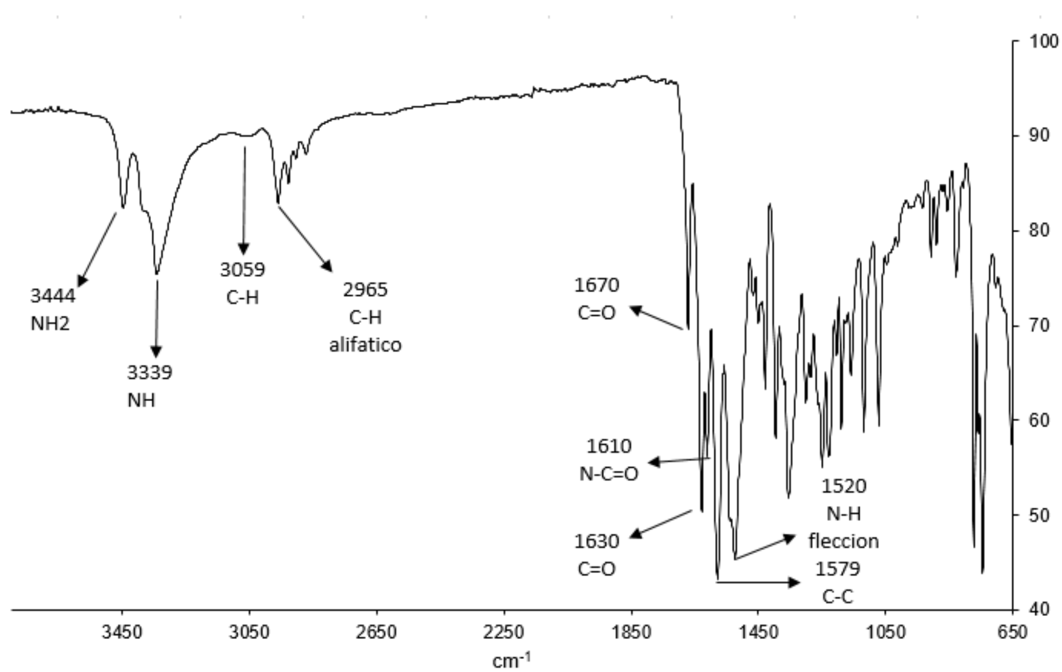

Figure S20. FTIR spectrum of **3b**.

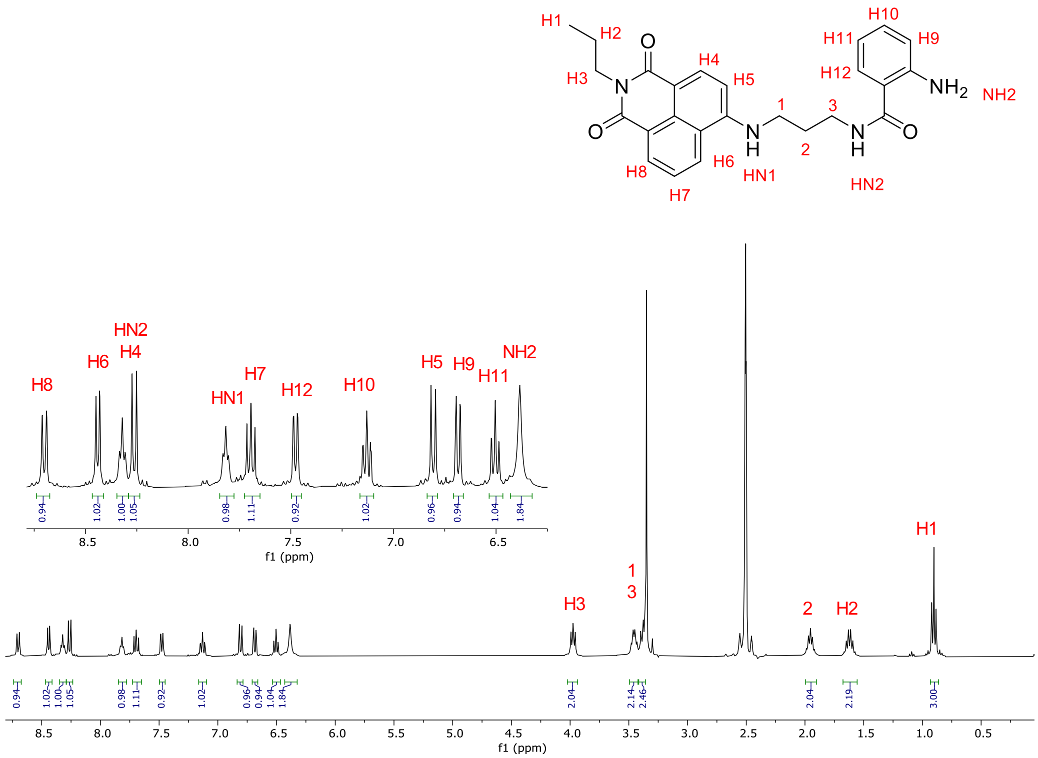

Figure S21. ^{1}H NMR spectrum of **3b** obtained in DMSO-d_6.

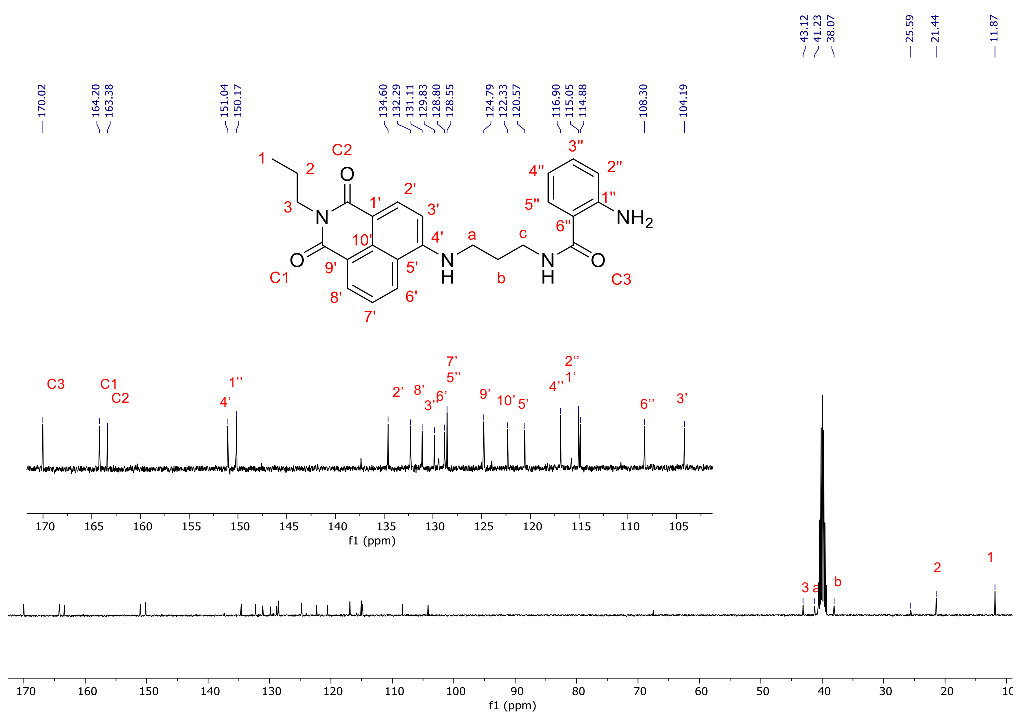

Figure S22. ^{13}C NMR spectrum of **3b** obtained in DMSO-d_6.

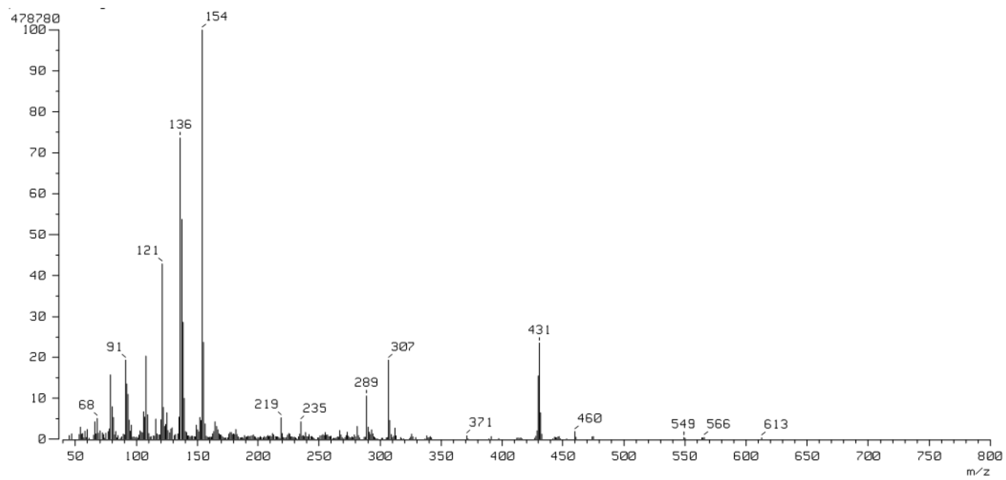

Figure S23. MS(FAB+) for **3b.**

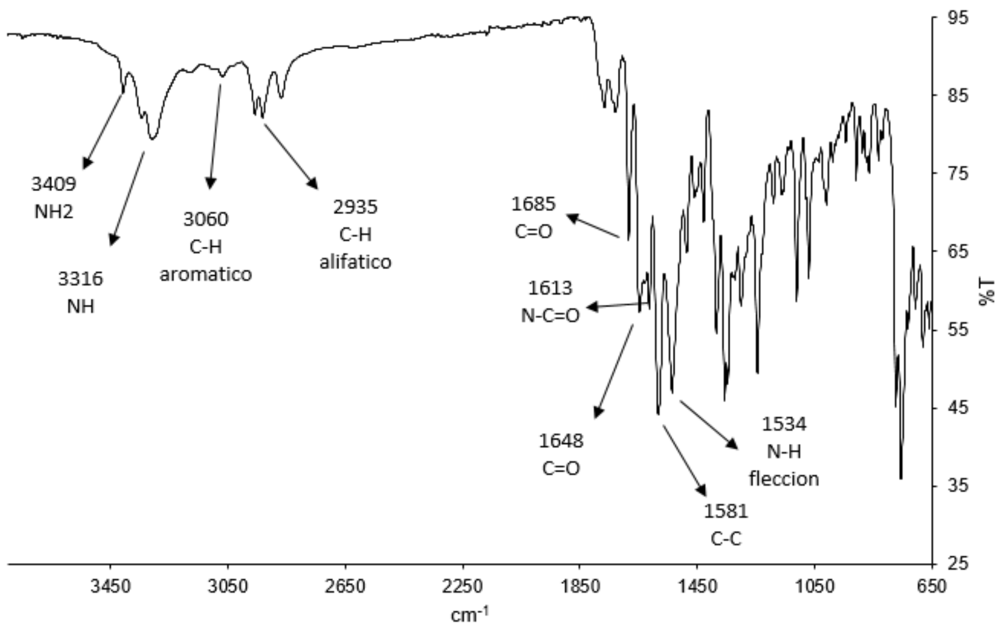

Figure S24. FTIR spectrum of **3c**.

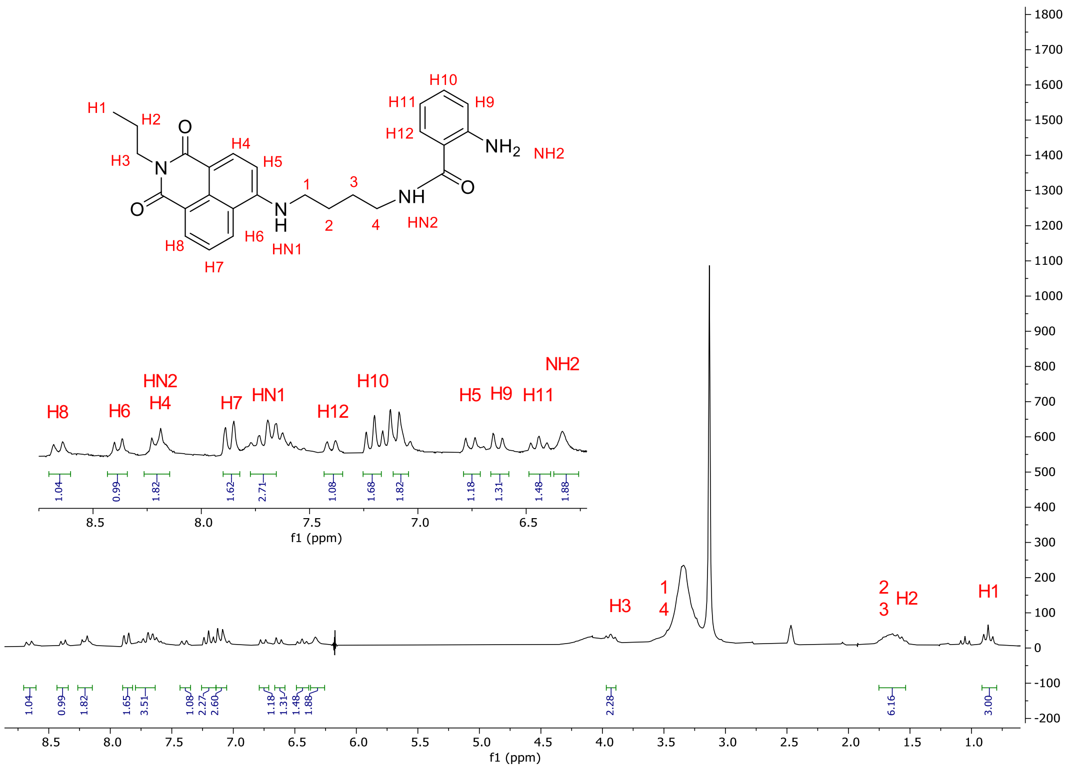

Figure S25. ^1H NMR spectrum of **3c** obtained in DMSO-d_6.

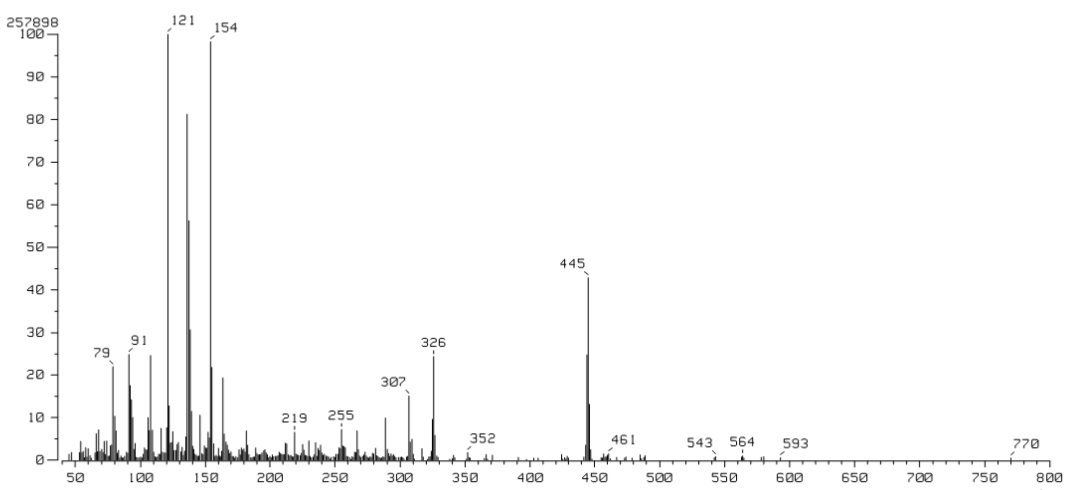

Figure S26. MS(FAB+) for **3c**.

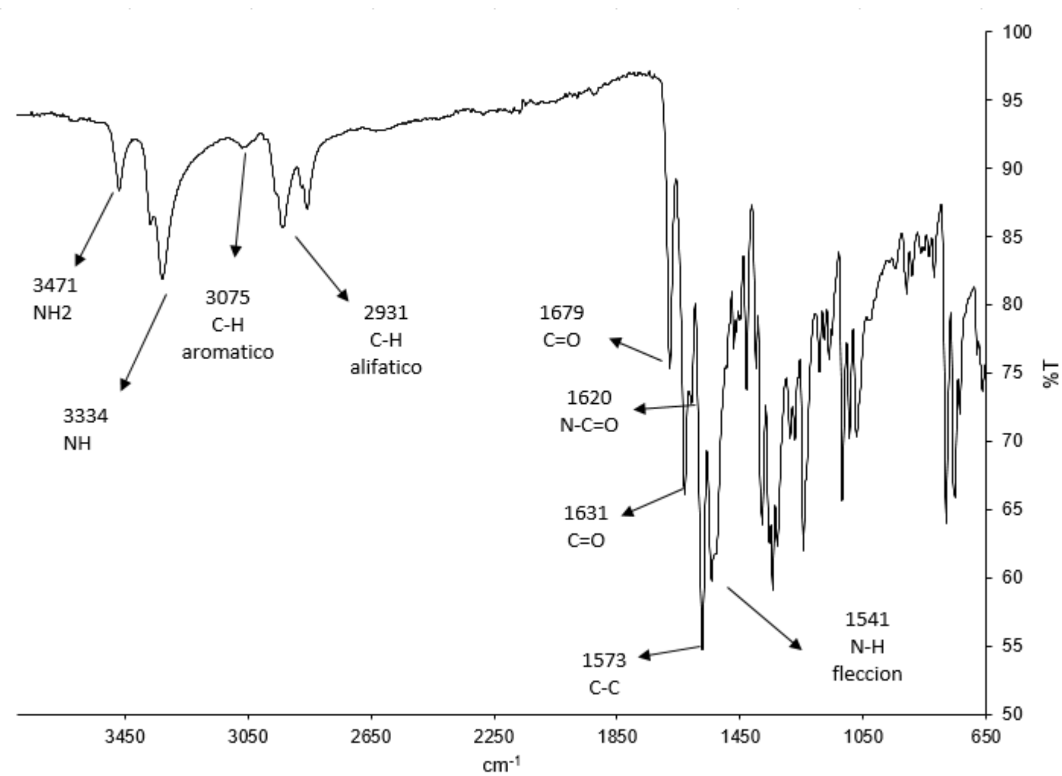

Figure S27. FTIR spectrum of **3d.**

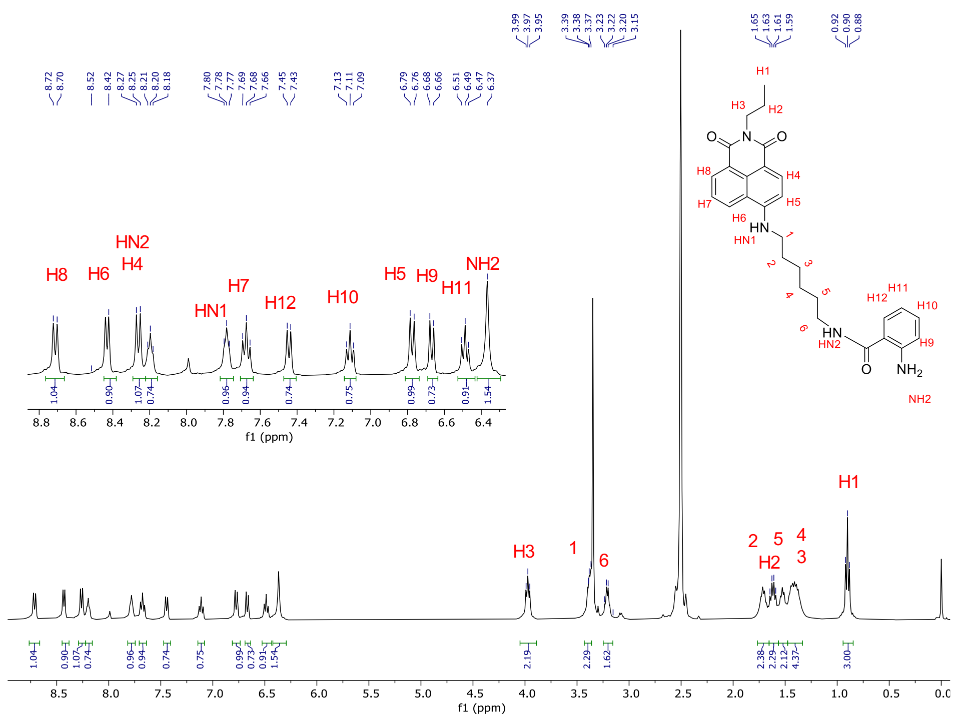

Figure S28. ^{1}H NMR spectrum of **3d** obtained in DMSO-d_6.

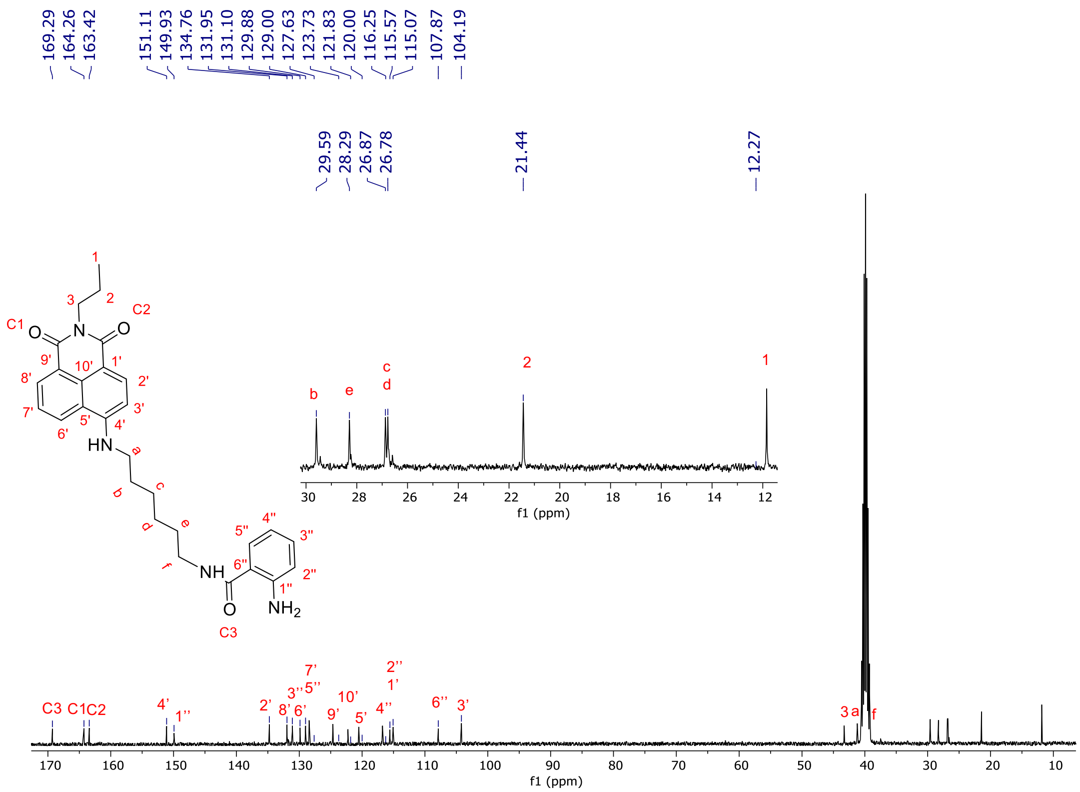

Figure S29. ^{13}C NMR spectrum of **3d** obtained in DMSO-d_6.

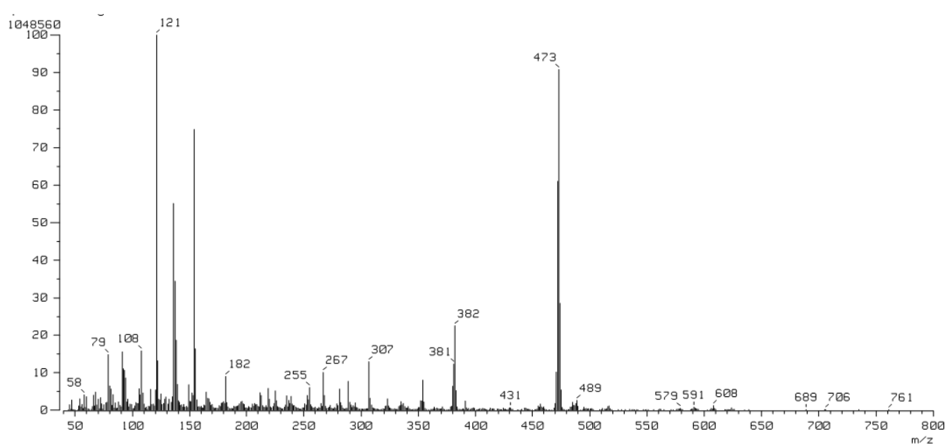

Figure S30. MS(FAB+) for **3d**.

Table S1. IR frequencies for dyads **3a-d** (cm^{-1}).

		(cm^{-1})			
	N-H	N-H	C-H	C-H	C=O
Dyad	Primary amine	Secundary amine	aromatic	aliphatic	symmetric
3a	3459	3349	3062	2956	1677
3b	3444	3339	3059	2965	1670
3c	3409	3316	3060	2935	1685
3d	3471	3334	3075	2931	1679
	N-C=O	**C=O**	**C=C**	**N-H**	
	amide	asymmetric	aromatic	bending	
3a	1615	1631	1578	1527	
3b	1610	1630	1579	1520	
3c	1613	1648	1581	1534	
3d	1620	1631	1573	1541	

Table S2. Assignation of ^{1}H NMR chemical shifts signals for compounds **3a-d**.

	3a		**3b**		**3c**		**3c**
^{1}H	(ppm)	**^{1}H**	(ppm)	**^{1}H**	(ppm)	**^{1}H**	(ppm)
H8	8.65 d	**H8**	8.70 d	**H8**	8.66 d	**H8**	8.71 d
HN2	8.49 t	**HN2**	8.32 t	**H6**	8.38 d	**H6**	8.43 d
H6	8.45 d	**H6**	8.44 d	**HN2**	8.21 s	**H4**	8.26 d
H4	8.28 d	**H4**	8.26 d	**H4**	8.18 d	**HN2**	8.20 t
HN1	7.94 t	**HN1**	7.82 t	**H7**	7.87 d	**HN1**	7.79 t
H7	7.71 t	**H7**	7.69 t	**HN1**	7.75 t	**H7**	7.68 t
H12	7.48 d	**H12**	7.48 d	**H12**	7.40 d	**H12**	7.44 d
H10	7.14 t	**H10**	7.13 ddd	**H10**	7.20 t	**H10**	7.11 t
H5	6.93 d	**H5**	6.81 d	**H5**	6.76 d	**H5**	6.78 d
H9	6.70 d	**H9**	6.68 dd	**H9**	6.63 d	**H9**	6.67 d
H11	6.51 t	**H11**	6.51 dd	**H11**	6.44 t	**H11**	6.49 t
NH2	6.45 s	**NH2**	6.38 s	**NH2**	6.33 s	**NH2**	6.37 s
H3	3.98 t	**H3**	3.97 t	**H3**	3.93 t	**H3**	3.98 t
1	3.55 s	**1**	3.46 m	**1**	3.4 m	**1**	3.36 m
2	3.55 s	**3**	3.36 m	**4**	3.28 m	**6**	3.21 c
H2	1.63 m	**2**	1.95 m	**2**	1.64 m	**2**	1.71 m
H1	0.91 t	**H2**	1.62 m	**3**	1.64 m	**H2**	1.63 m
		H1	0.90 t	**H2**	1.63 m	**5**	1.53 m
				H1	0.91 t	**4**	1.4 m
						3	1.4 m
						H1	0.91 t

Table S3. Assignation of ^{13}C NMR chemical shifts signals for compounds **3a-d**..

Dyad	amide	imide	aromatic	propyl	alkyl spacer
3a	170.02	164.20, 163.38	151.04, 150.17, 134.60, 132.29, 131.11, 129.83, 128.80, 128.55, 124.79, 122.33, 120.57, 116.90, 115.05, 114.88, 108.30, 104.19	43.12, 21.44, 11.87.	41.23, 38.07
3b	170.09	164.27, 163.45	151.11, 150.24, 134.67, 132.36, 131.18, 129.9, 128.87, 128.62, 124.86, 122.4 120.64, 116.83 114.98, 114.81, 108.23, 104.12	43.05 21.37 11.8	41.16, 38.12, 28.34
3d	169.29	164.29, 163.42	151.11, 149.93, 134.76, 131.95, 131.10, 129.88, 129.00, 128.43, 124.65, 122.25, 120.53, 116.75, 115.57, 115.07, 107.87, 104.19,	43.28, 21.44, 11.85.	41.20, 39.18, 29.59, 28.29, 26.87, 26.78

.

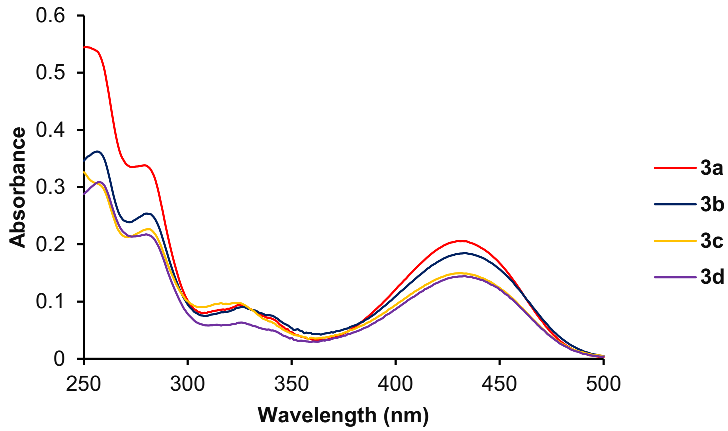

Figure S31. Electronic absorption bands of dyads **3a-d** in acetonitrile. [**3a-d**]= 1×10^{-5} M.

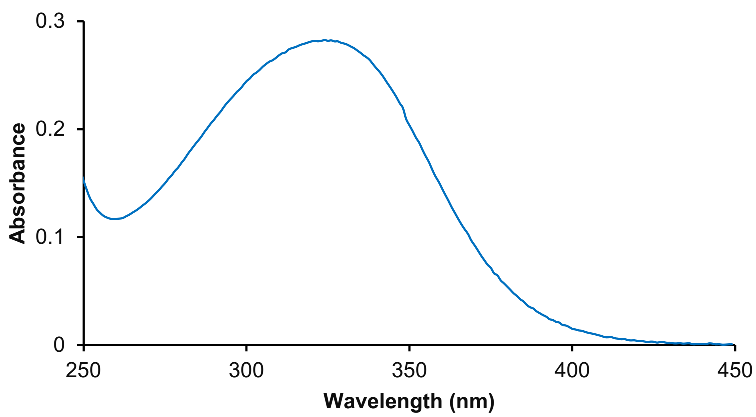

Figure S32. Electronic absorption band of $Cu(ClO_4)_2$ in acetonitrile. [$Cu(ClO_4)_2$]= 1×10^{-4} M.

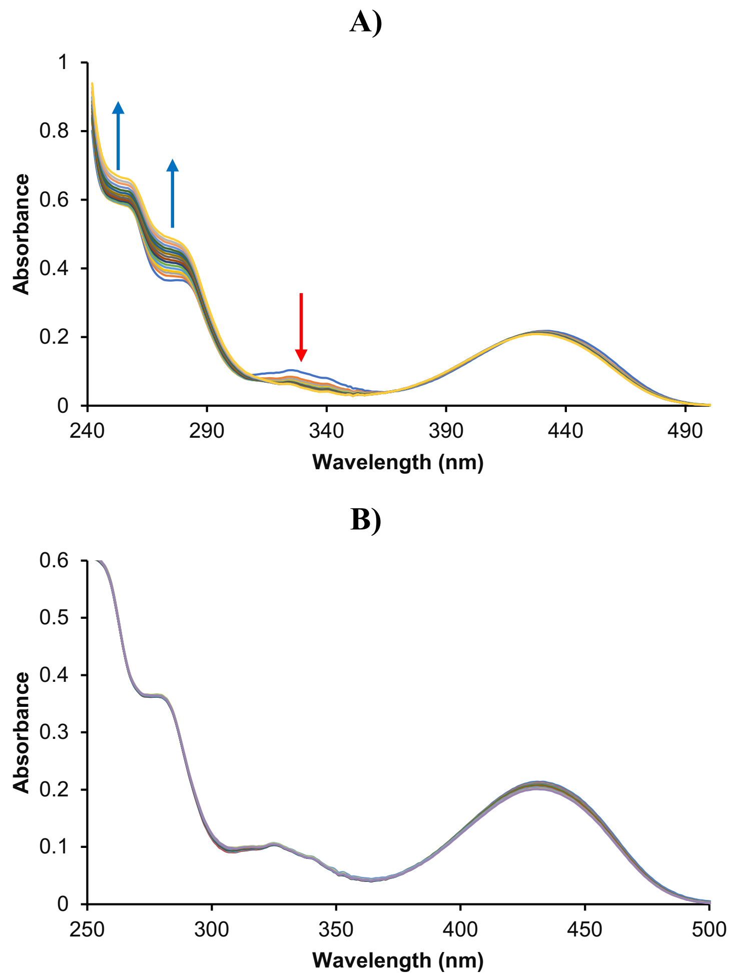

Figure S33. Absorption spectra obtained by titration of dyad **3a** with Hg^{2+} (A) and Cu^{2+} (B) in acetonitrile. [**3a**]= 1×10^{-5} M.

A)

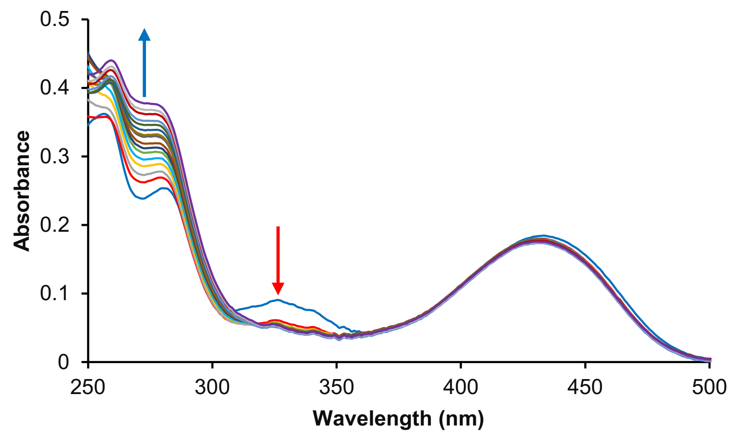

B)

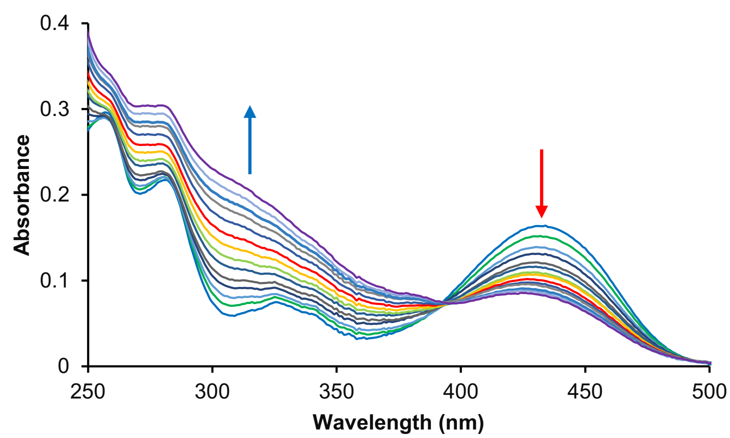

Figure S34. Absorption spectra obtained by titration of dyad **3b** with Hg^{2+} (A) and Cu^{2+} (B) in acetonitrile. [**3b**]= 1×10^{-5} M.

A)

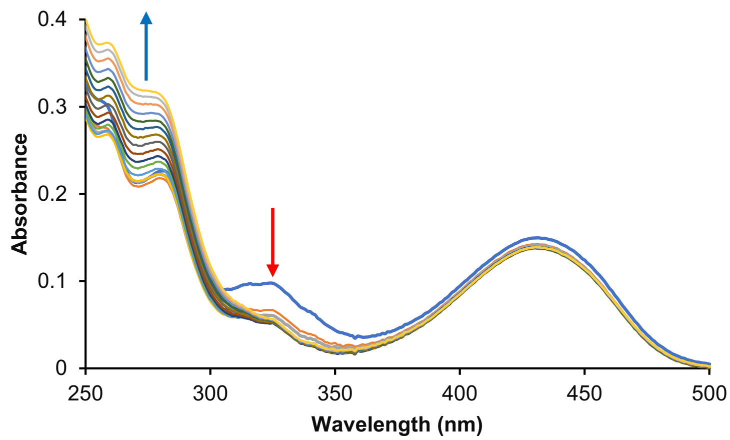

B)

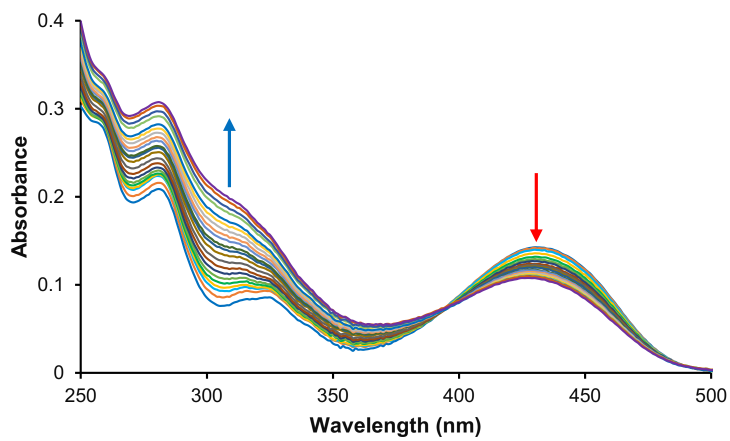

Figure S35. Absorption spectra obtained by titration of dyad **3c** with Hg^{2+} (A) and Cu^{2+} (B) in acetonitrile. [**3c**]= 1×10^{-5} M.

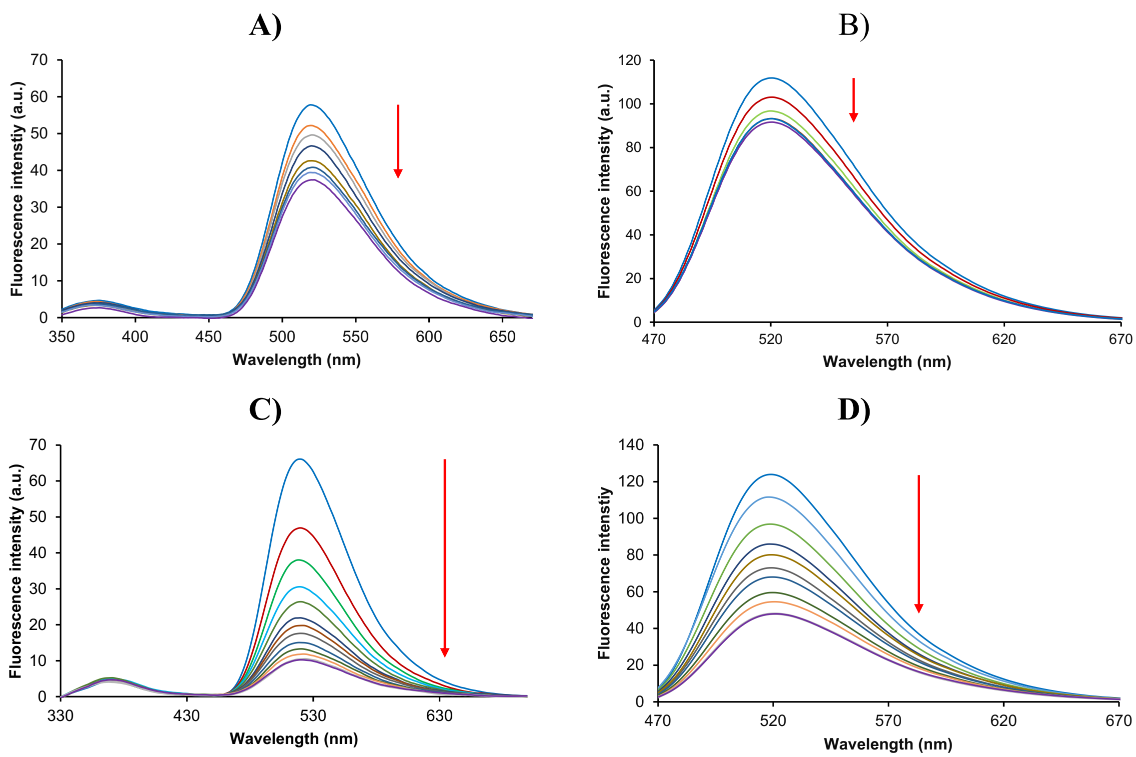

Figure S36. Emission spectra obtained by titration of dyad **3a** with Cu^{2+} exciting at 315 nm (A) and 435 nm (B) in acetonitrile. Emission spectra obtained by titration of dyad **3a** with Hg^{2+} exciting at 315 nm (C) and 435 nm (D) in acetonitrile. [**3a**]= $5{\times}10^{-5}$ M.

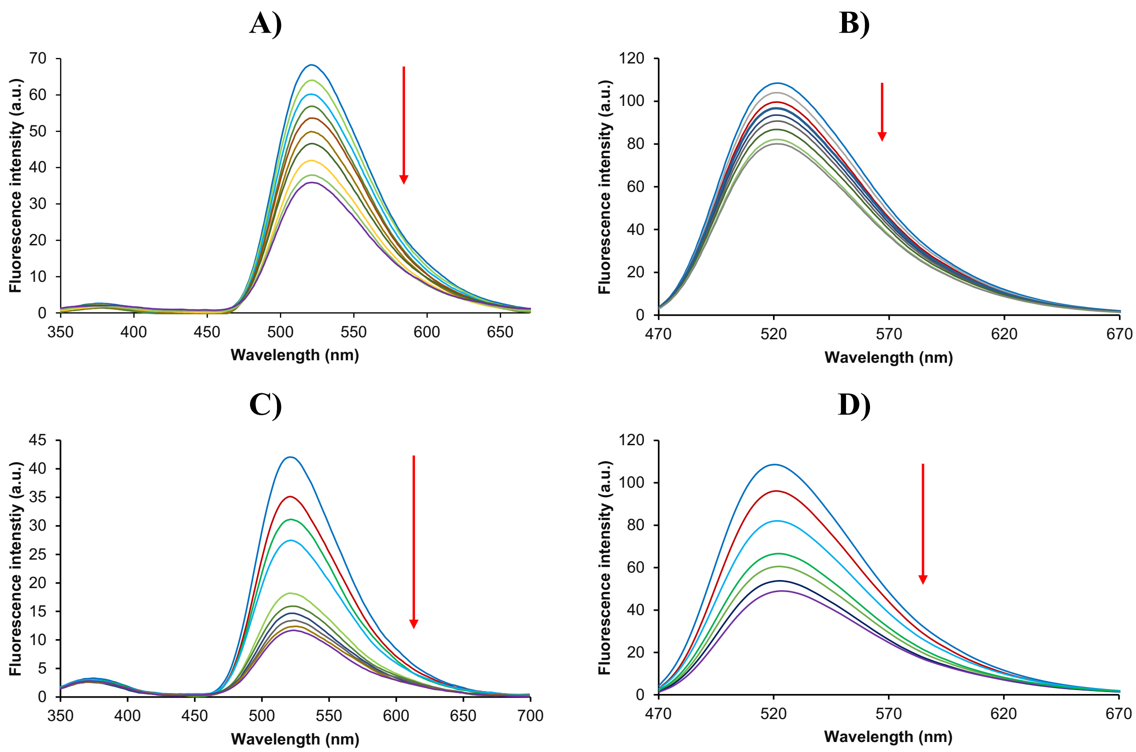

Figure S37. Emission spectra obtained by titration of dyad **3b** with Cu^{2+} exciting at 315 nm (A) and 435 nm (B) in acetonitrile. Emission spectra obtained by titration of dyad **3b** with Hg^{2+} exciting at 315 nm (C) and 435 nm (D) in acetonitrile. [**3b**]= 5×10^{-5} M.

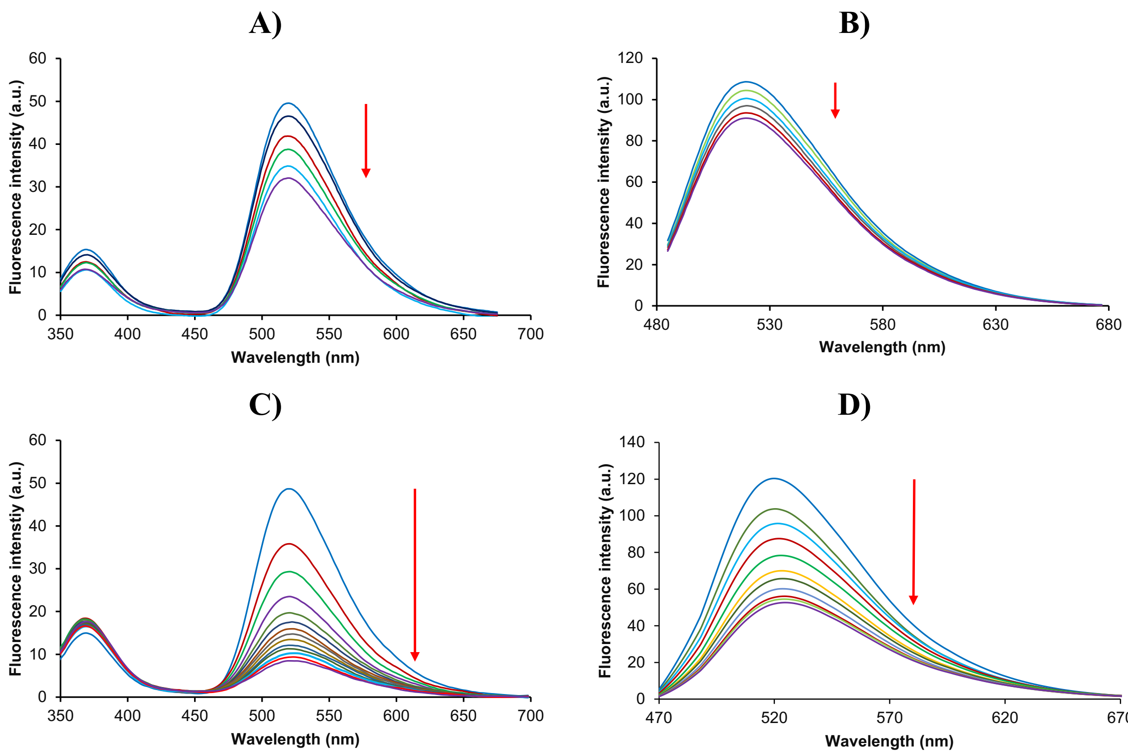

Figure S38. Emission spectra obtained by titration of dyad **3c** with Cu^{2+} exciting at 315 nm (A) and 435 nm (B) in acetonitrile. Emission spectra obtained by titration of dyad **3c** with Hg^{2+} exciting at 315 nm (C) and 435 nm (D) in acetonitrile. [**3c**]= 5×10^{-5} M.

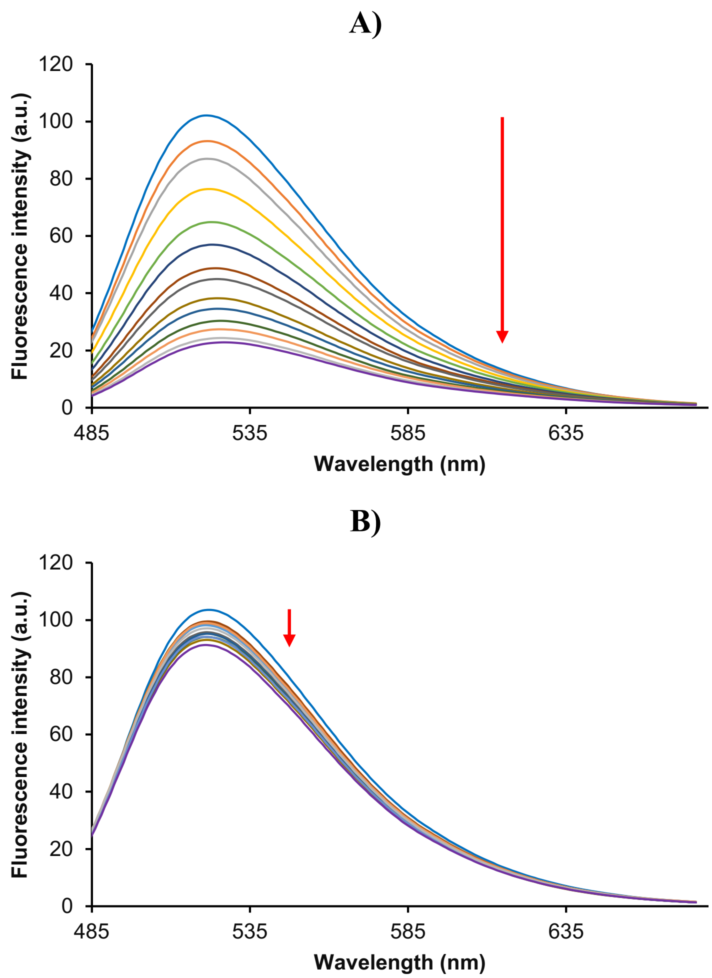

Figure S39. Emission spectra obtained by titration of **pp-ANAPIM** with Hg^{2+} (A) and Cu^{2+} (B) in acetonitrile. [**pp-ANAPIM**]= 5×10^{-5} M, λ_{ex}= 450 nm.

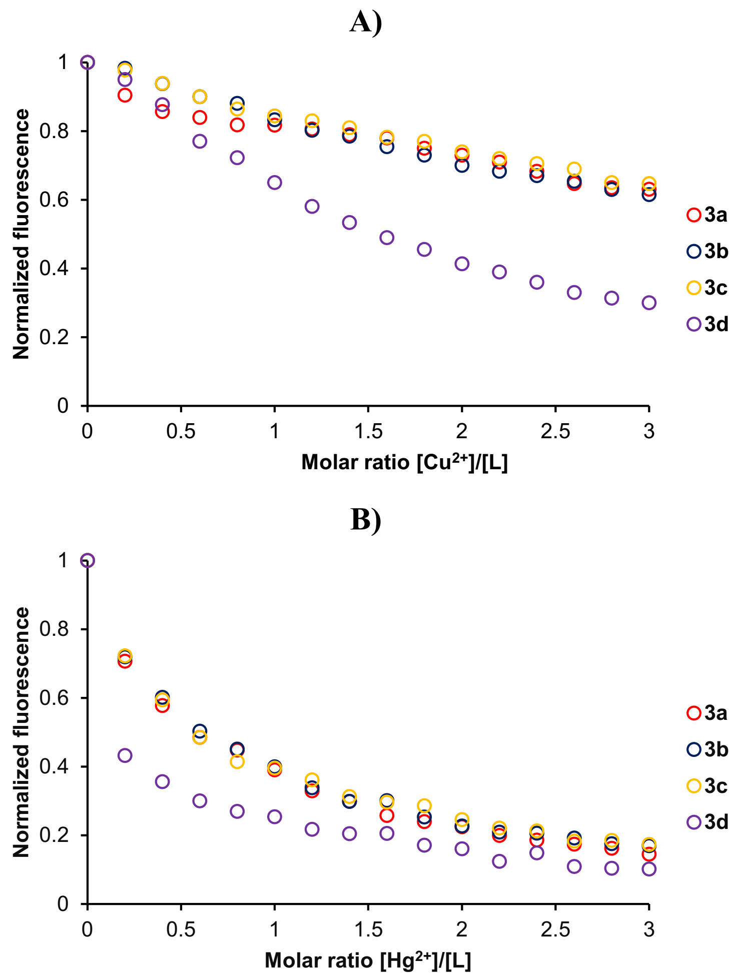

Figure S40. Normalized fluorescent profiles obtained by titration of dyads **3a-d** with Cu^{2+} (A) and Hg^{2+} (B) in acetonitrile. λ_{ex}= 315 nm. [**3a-d**]= 5×10^{-5} M.

A)

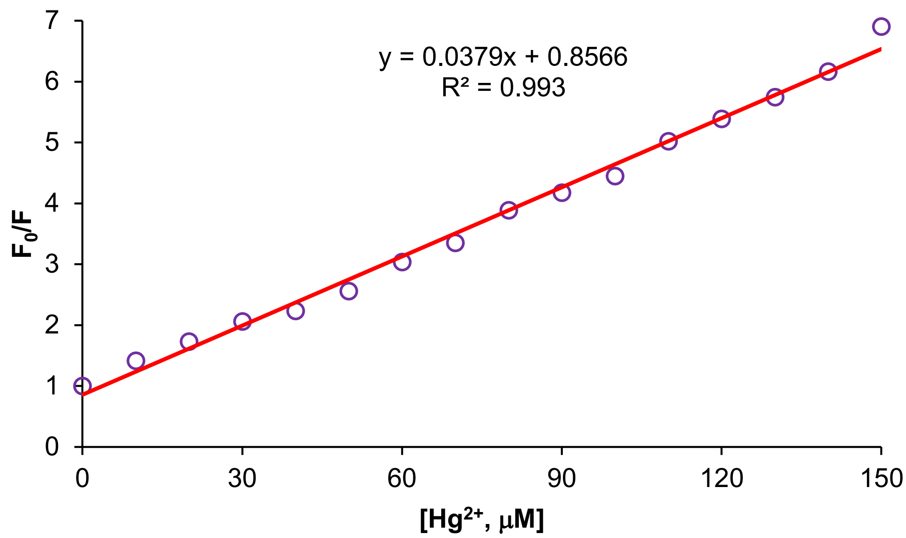

B)

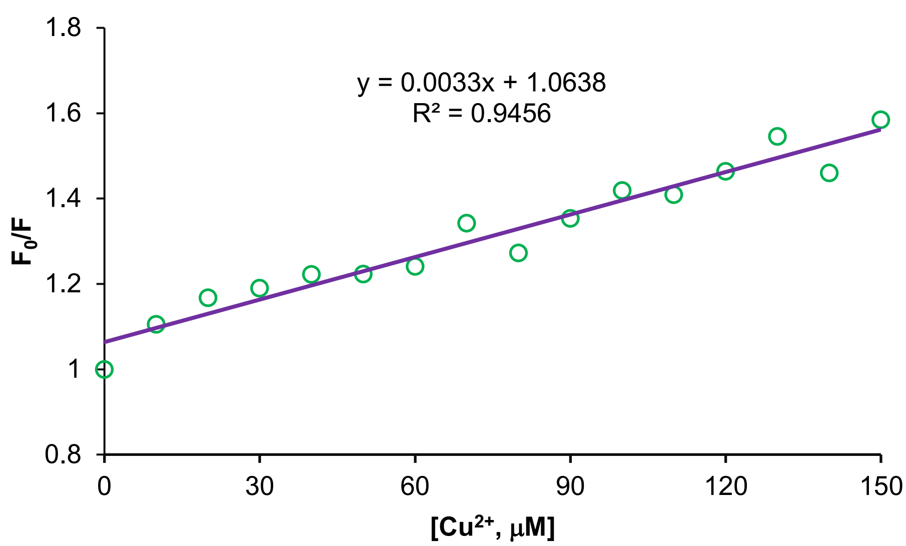

Figure S41. Stern-Volmer graph obtained from the emission of **3a** with Hg^{2+} (A) and Cu^{2+} (B) exciting at 315 nm in acetonitrile. [**3a**]= 5×10^{-5} M.

A)

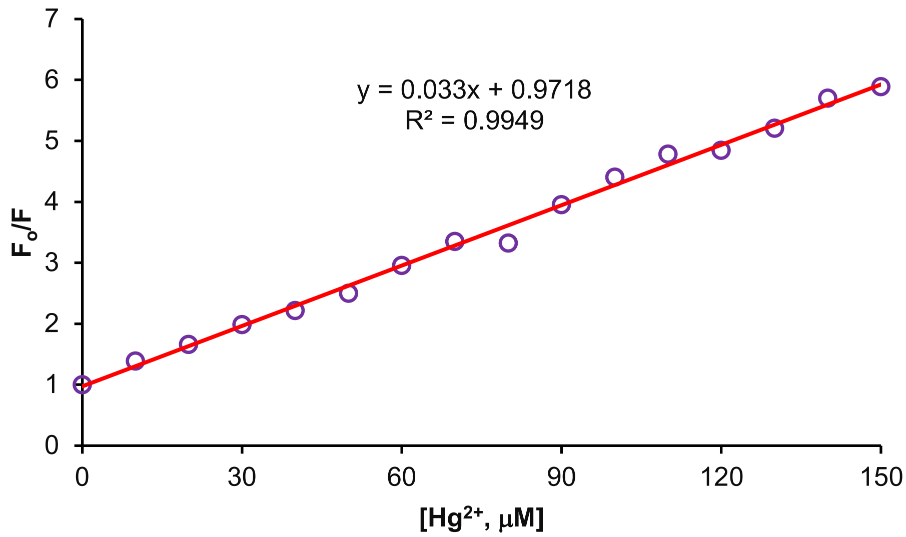

B)

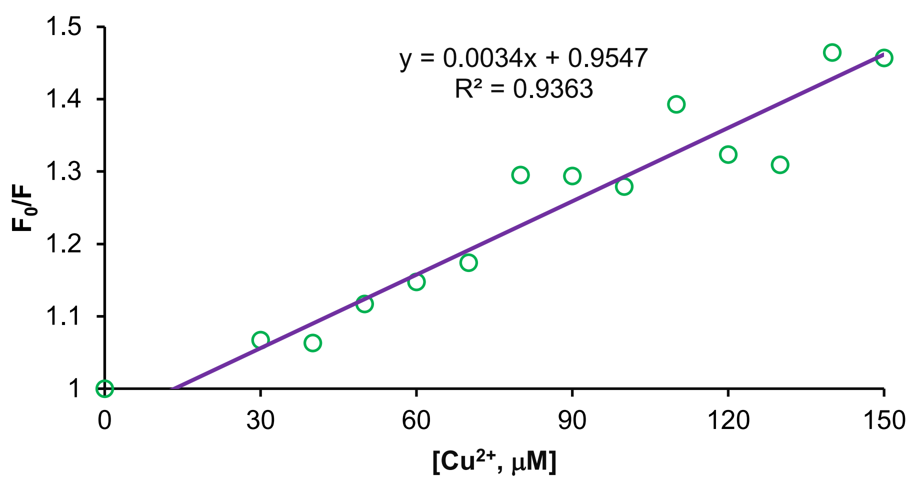

Figure S42. Stern-Volmer graph obtained from the emission of **3b** with Hg^{2+} (A) and Cu^{2+} (B) exciting at 315 nm in acetonitrile. [**3b**]= 5×10^{-5} M.

A)

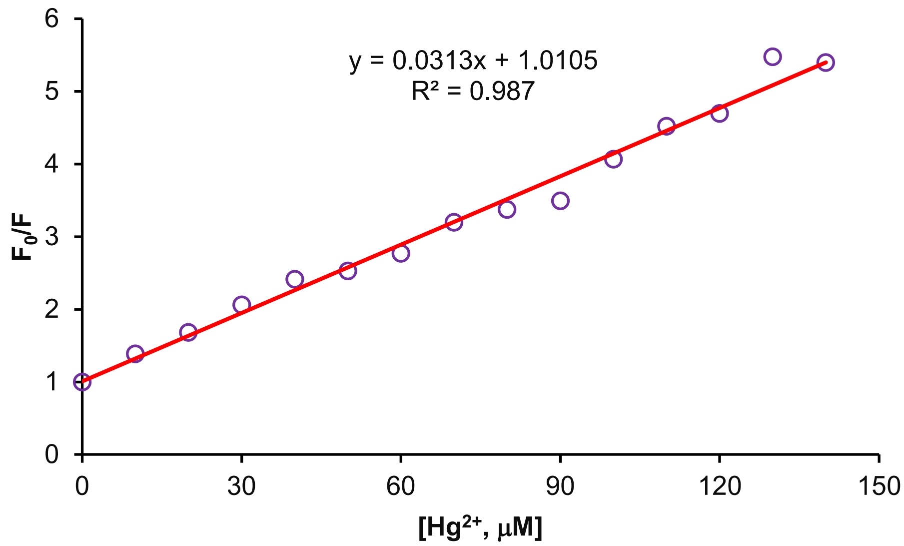

B)

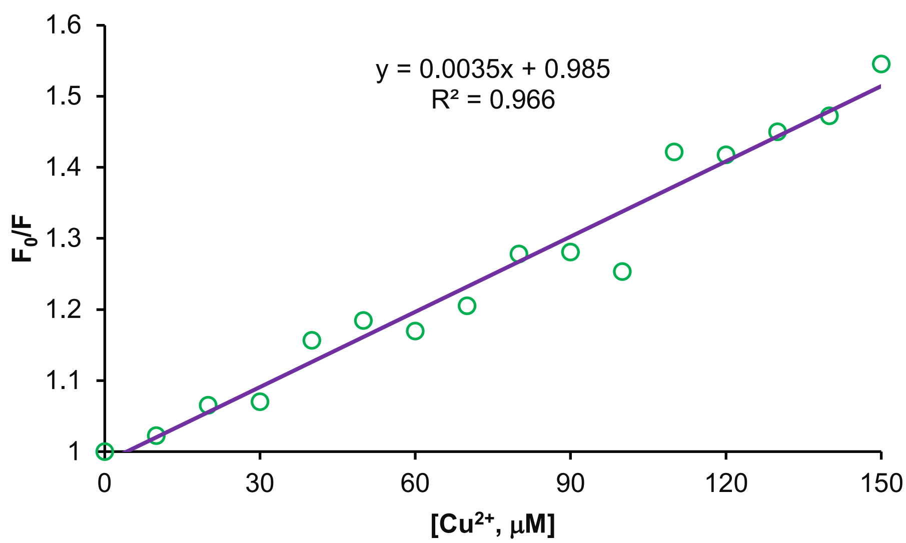

Figure S43. Stern-Volmer graph obtained from the emission of **3c** with Hg^{2+} (A) and Cu^{2+} (B) exciting at 315 nm in acetonitrile. [**3c**]= 5×10^{-5} M.

A)

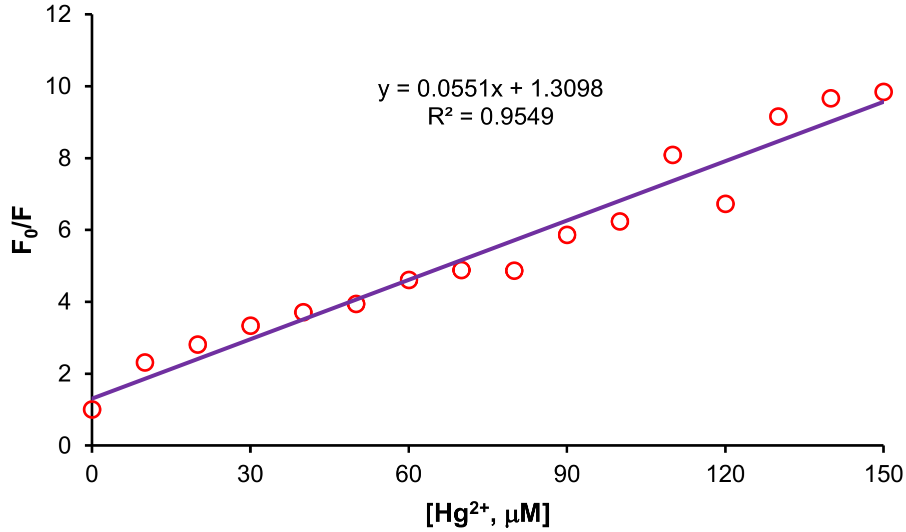

B)

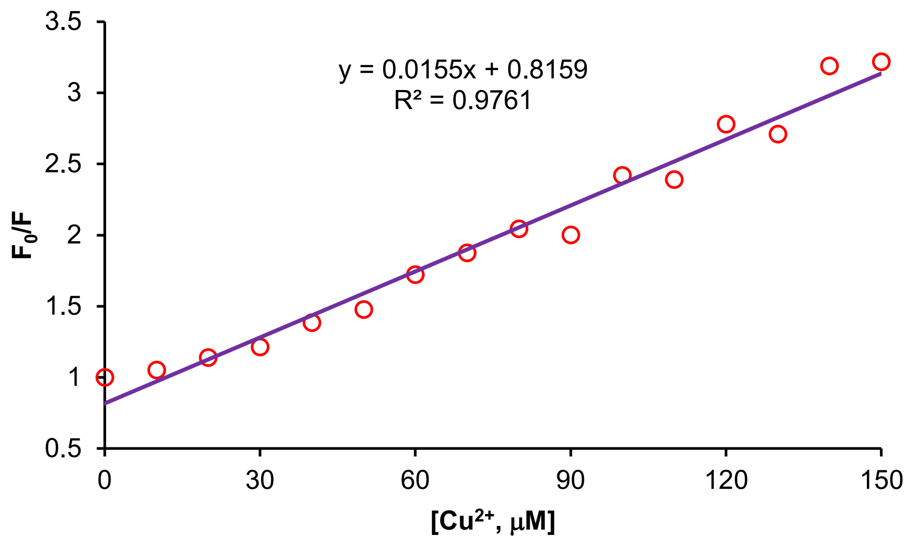

Figure S44. Stern-Volmer graph obtained from the emission of **3d** with Hg^{2+} (A) and Cu^{2+} (B) exciting at 315 nm in acetonitrile. [**3d**]= 5×10^{-5} M.

Table S4. Fluorescence quenching percentages in the complexes prepared with **3a-d**.

Cation	**Hg(II)**	**Hg(II)**	**Cu(II)**	**Cu(II)**
λ_{ex}	315 nm	435 nm	315 nm	435 nm
3a	86%	61%	39%	19%
3b	83%	54%	31%	5%
3c	83%	49%	31%	11%
3d	90%	77%	69%	51%

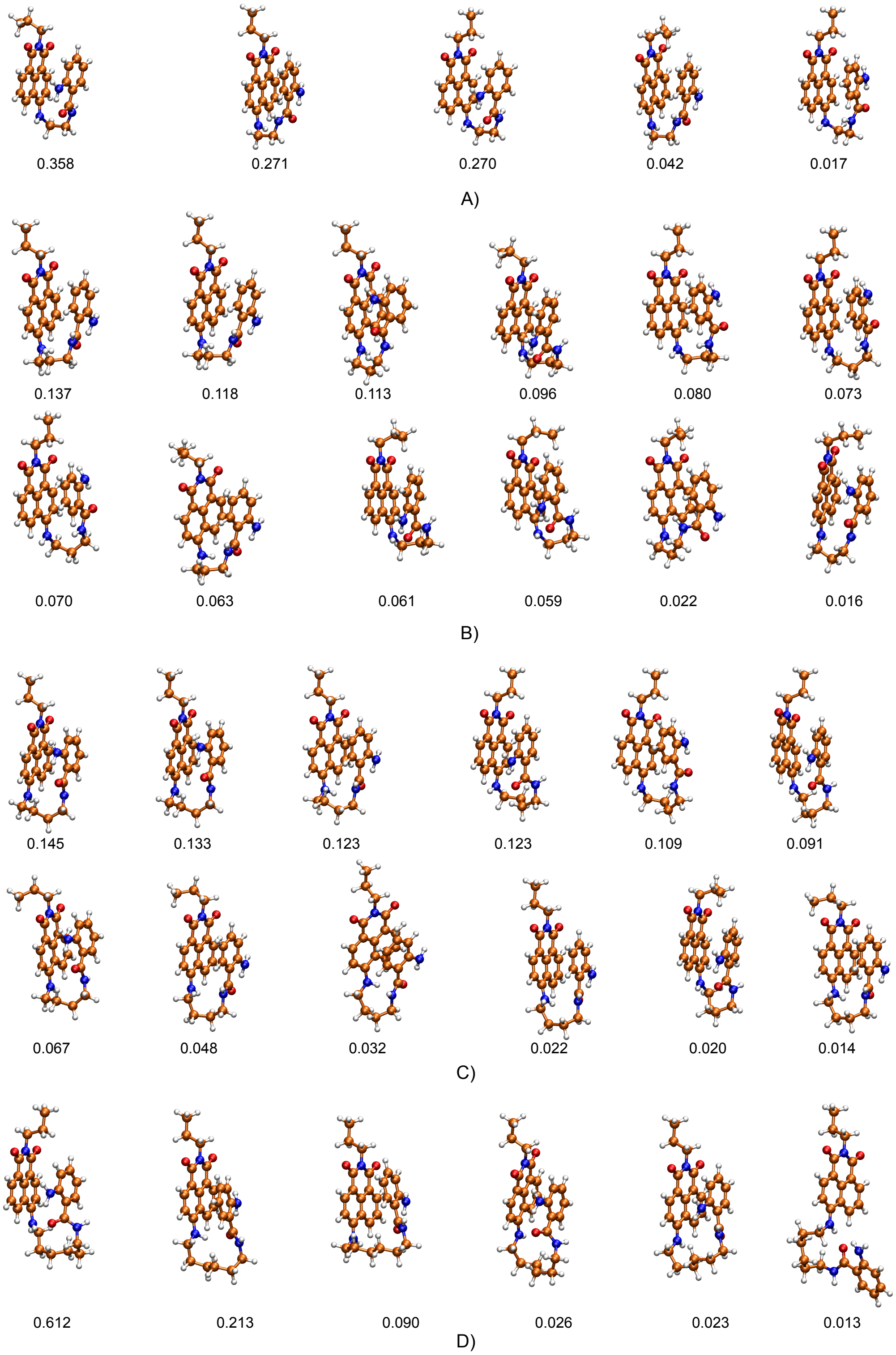

Figure S45. Lateral view of the most relevant conformations for the dyads 3a (a), 3b (b), 3c (b) and 3b (d). The numbers below the structures correspond to the Boltzmann factors evaluated at 298 K.

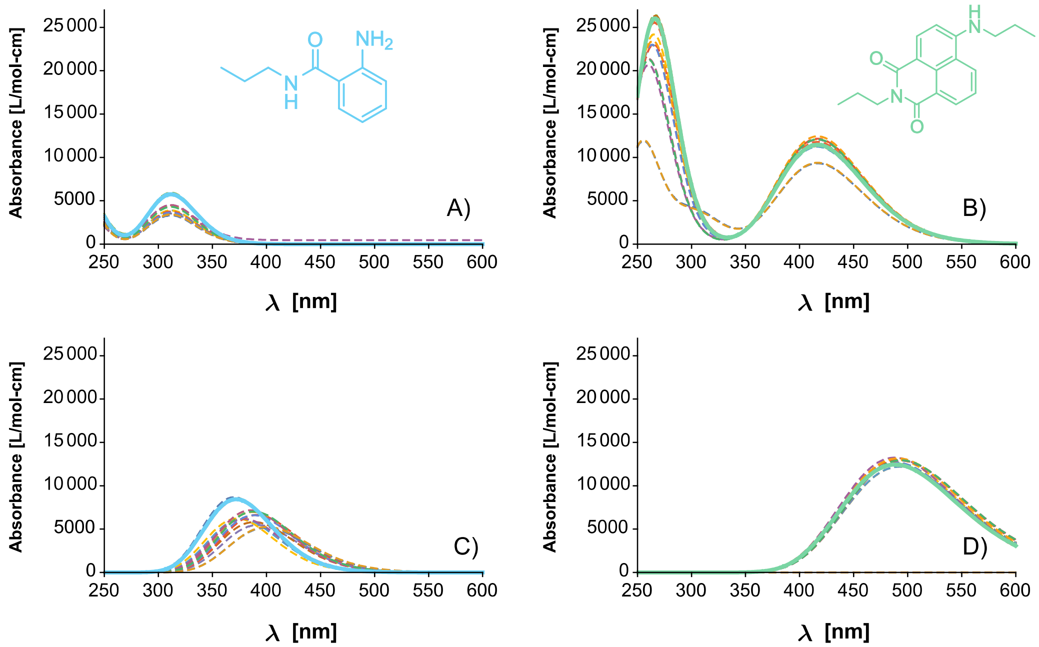

Figure S46. Simulated electronic absorption (A and B) and emission (C and D) spectra of p-2ABZ and pp-ANAPIM considering the Boltzmann average between the thermally allowed conformations (weights >0.01) at 298 K. The vertical electronic transitions are convoluted with Gaussian functions with a half width of 0.4 eV. Dashed lines correspond to the conformer contributions, whilst the color solid line corresponds to the average value.

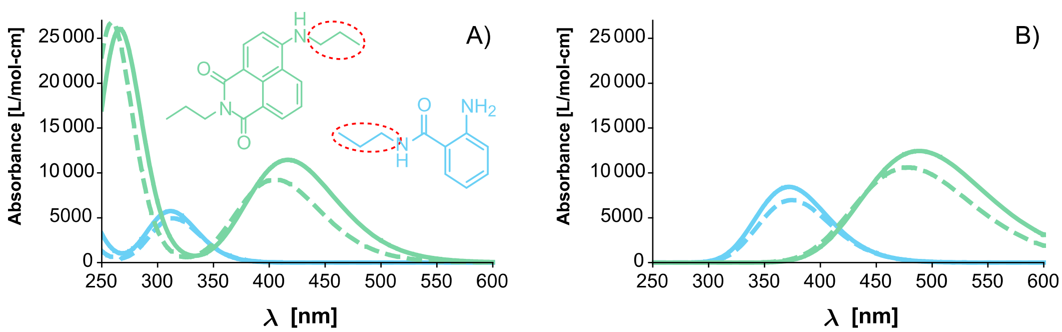

Figure S47. (A) Simulated electronic absorption and emission spectra for **p-2ABZ** and **pp-ANAPIM** (solid lines) and (B) their non-alkylated analogues (dashed lines). The values consider the Boltzmann average at 298 K. The vertical electronic transitions where convoluted with Gaussian functions with a half width of 0.4 eV.

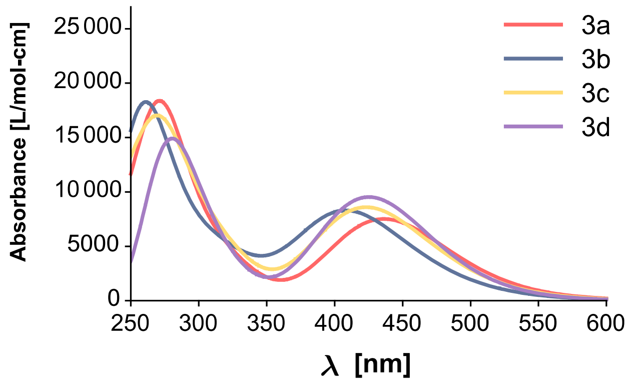

Figure S48. Simulated electronic spectra for dyads **3a-d**. The values consider the Boltzmann average at 298 K. The vertical electronic transitions are convoluted with Gaussian functions with half width of 0.4 eV.

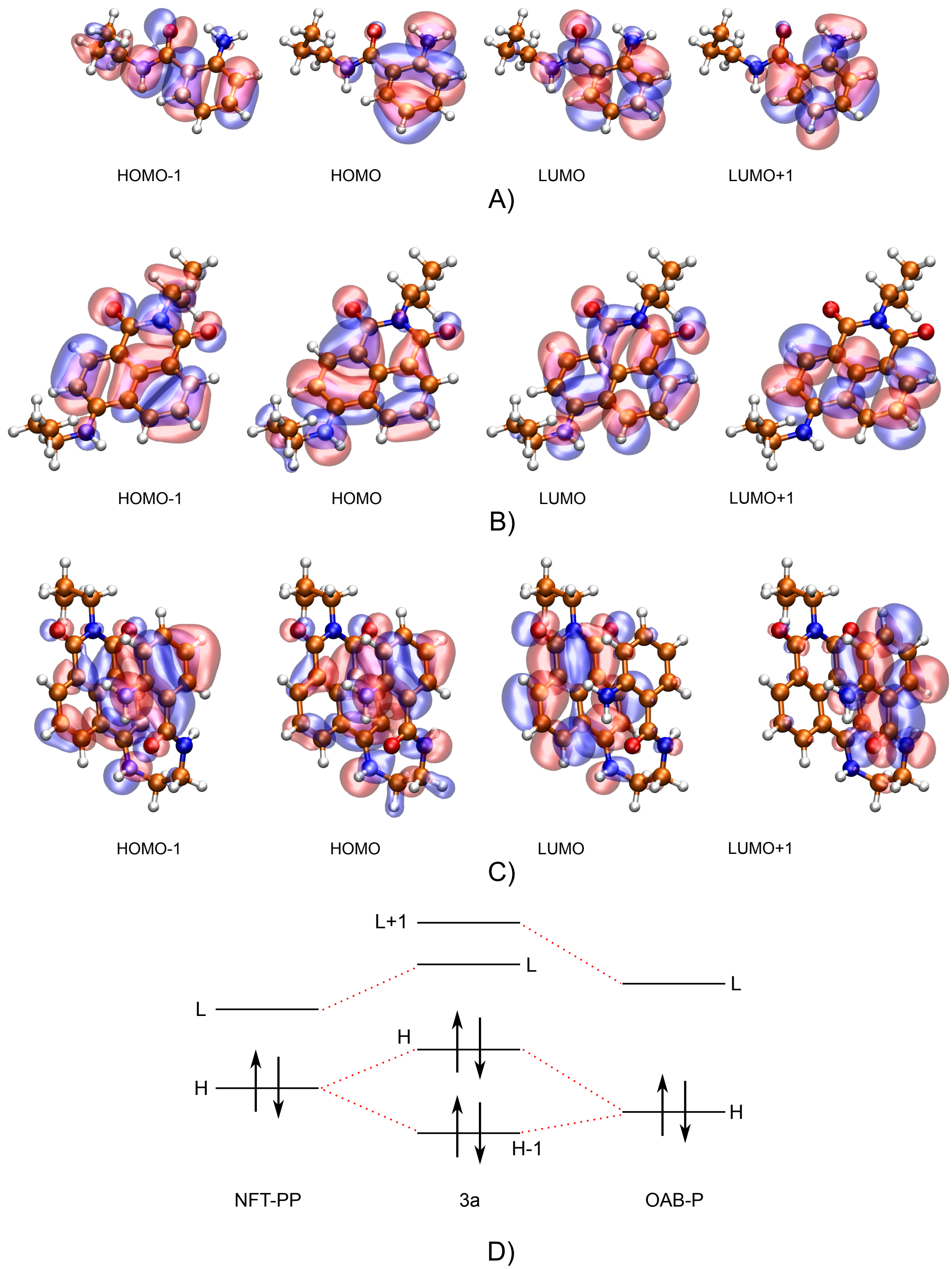

Figure S49. Isosurface (|0.02|) of the boundary molecular orbitals for the **p-2AZO** (a), **PP-ANAPIM** (b) and **3a** (c) molecules. (d) Sketch of the correlation diagram for the formation of **3a** from **p-2AZO** and **PP-ANAPIM**.

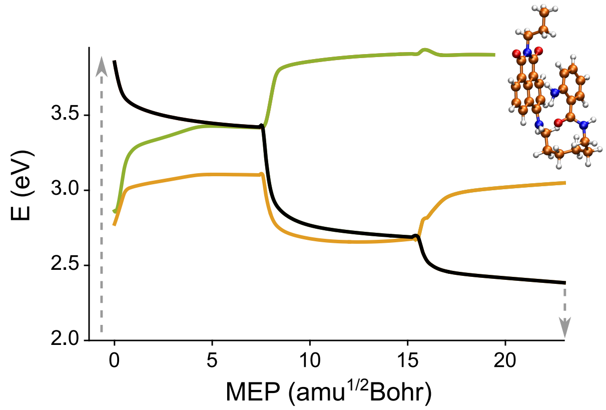

Figure S50. Energy of the first singlet electronic states along the minimum energy path in the exciting state of stacked (A) and folded (B) conformations of **3a**. The vertical dotted lines denote a vertical transition from/to the S_0.

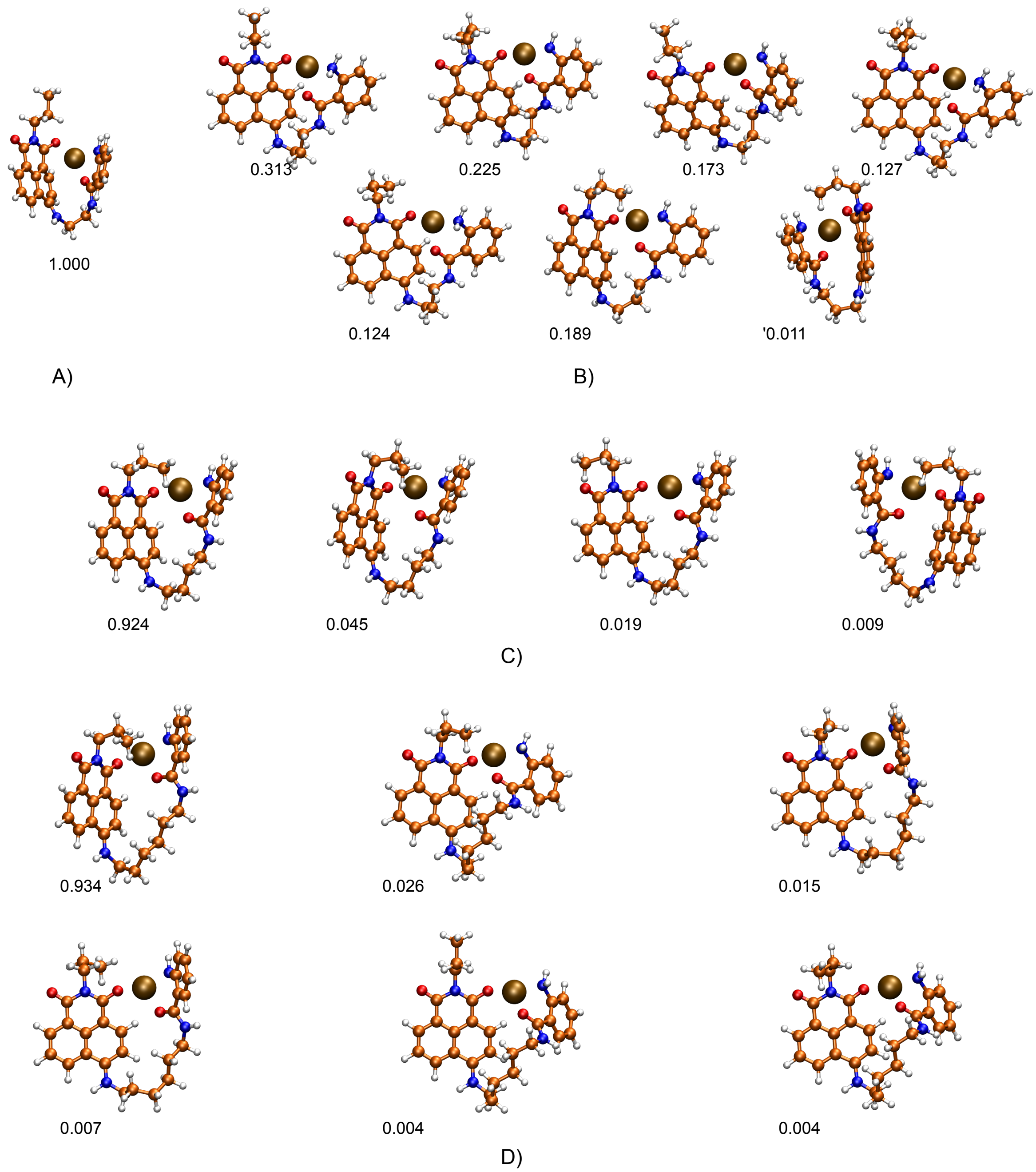

Figure S51. Side view of the most relevant conformations for the complexes formed by Cu^{+2} and dyads 3a (a), 3b (b), 3c (c) and 3d (d). The numbers below the structures correspond to the Boltzmann factors evaluated at 298 K.

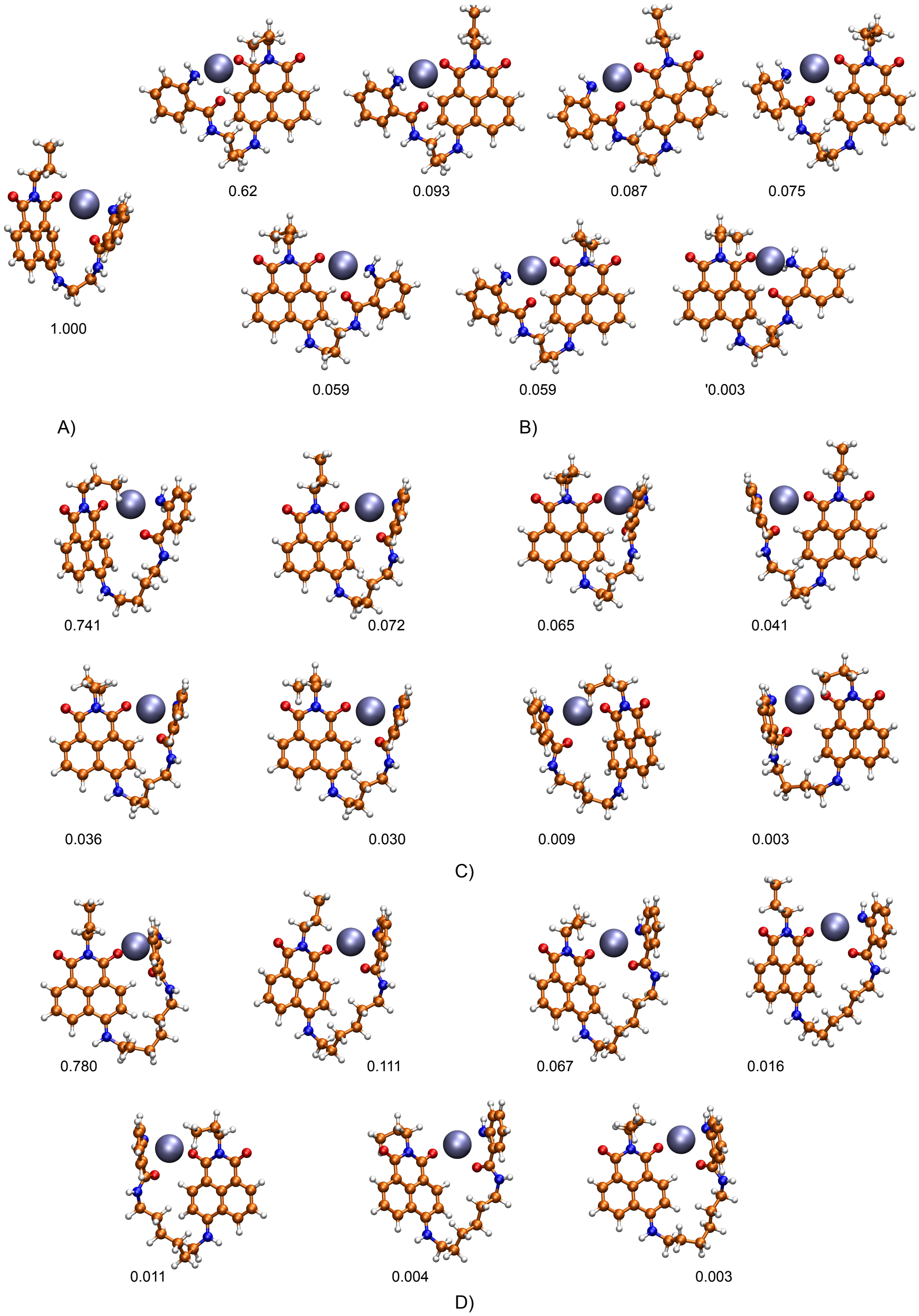

Figure S52. Side view of the most relevant conformations for the complexes formed by Hg^{+2} and dyads 3a (a), 3b (b), 3c (c) and 3d (d). The numbers below the structures correspond to the Boltzmann factors evaluated at 298 K.

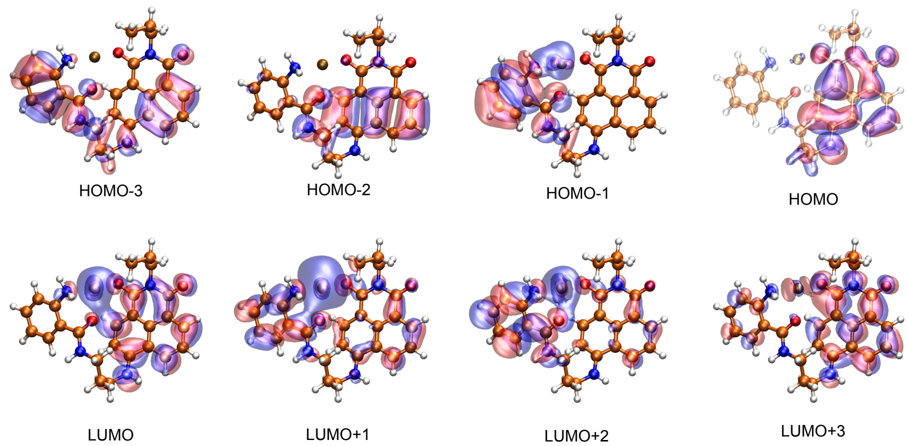

Figure S53. Isosurface (|0.02|) of the boundary molecular orbitals for the **Hg^{+2}-3a** complex. The structure corresponds to the global minima.

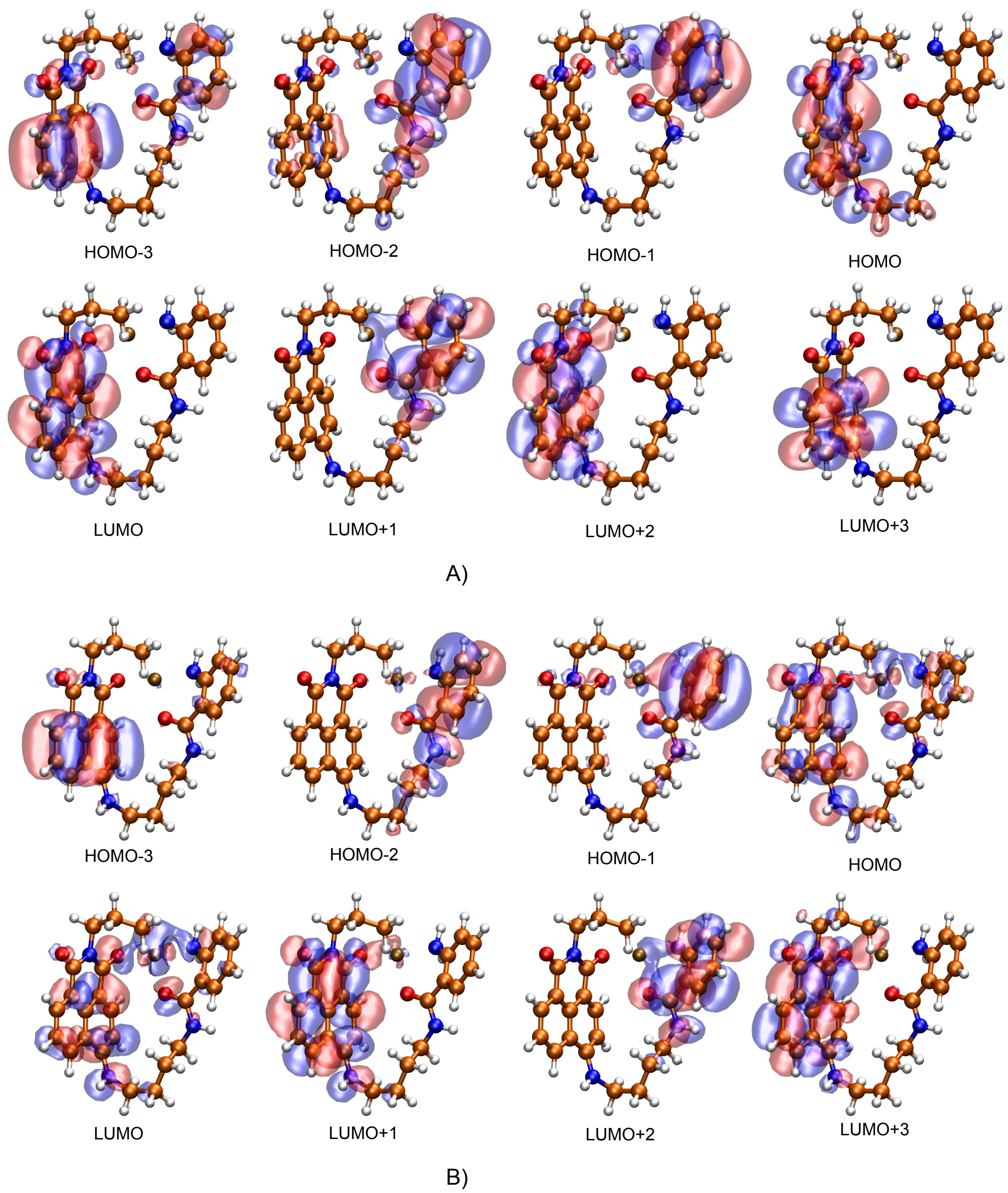

Figure S54. Isosurface (|0.02|) of the boundary molecular orbitals alfa (A) and beta (B) for the **Cu^{+2}-3a** complex. The structure corresponds to the global minima.

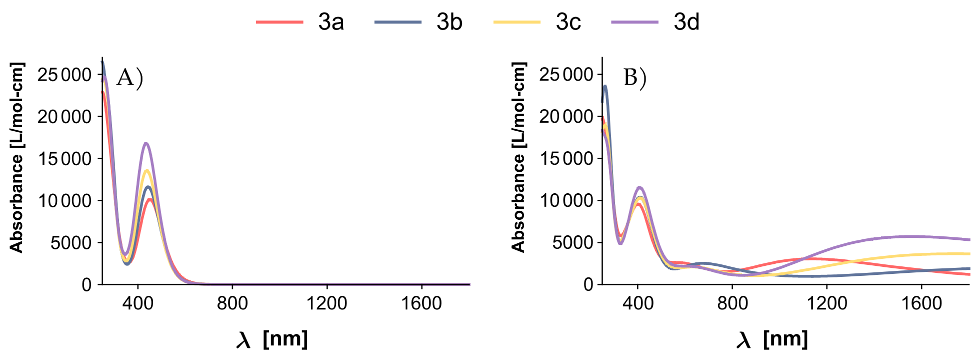

Figure S55. Simulated electronic spectra for the complexes of Hg^{+2} (A) and Cu+2 (B) with the dyads **3a-d**. The values consider the Boltzmann average at 298 K. The vertical electronic transitions are convoluted with Gaussian functions with half width of 0.4 eV